Dynamic Volt-Watt Control Strategy to Improve Fairness While Mitigating Overvoltage in Distribution System due to High Penetration of PV

by

Shafait Ahmed

BScEEE, International Islamic University Chittagong, 2011

A Thesis Submitted in Partial Fulfillment of
the Requirements for the Degree of

Master of Science in Engineering

in the Graduate Academic Unit of Electrical and Computer Engineering

Supervisor (s): Chris Diduch, PhD, Electrical & Computer Engineering
Julian Cardenas Barrera, PhD, Electrical & Computer Engineering

Examining Board: Brent Petersen, PhD, Electrical & Computer Engineering, Chair
Trevor Robin Hanson, PhD, Civil Engineering
Liuchen Chang, PhD, Electrical & Computer Engineering

This thesis is accepted by the Dean of Graduate Studies

THE UNIVERSITY OF NEW BRUNSWICK

December 2024

Abstract

The risk of overvoltage problems due to high penetration of distributed generation is a growing issue in low-voltage distribution networks. The use of Smart Inverters (SI) in the distribution system can help regulate voltage by controlling active and reactive power generation through volt-watt and volt-var droop control strategies. Conventional volt-watt and volt-var control methods use static parameters, which can lead to unnecessary curtailment of photovoltaics (PV) power, lower power factor, and/or reduction in PV hosting capacity. We propose two different algorithms that dynamically shape the volt-watt curve based on the voltage sensitivity of the PV nodes. Unlike centralized approaches, we adopt a distributed control strategy that minimizes reliance on extensive communication infrastructure, thereby improving system resilience. The proposed methods are simple to implement and require minimal communication among system components, enabling effective local control without the complexity of centralized coordination. To assess the performance of the proposed algorithms, we used the IEEE 37-bus system as a test network. Simulation results confirm the effectiveness of these strategies in enhancing fairness in PV curtailment and reducing overall curtailment levels. The proposed methods were implemented and evaluated through a co-simulation platform integrating the OpenDSS power simulator and Python, demonstrating their practical applicability and robustness in a simulated distribution system environment.

Acknowledgements

This thesis project was carried out under the supervision of Dr. Chris Diduch and Dr. Julian Cardenas Barrera from the Electrical and Computer Engineering Department, University of New Brunswick (UNB). I extend my deepest gratitude to my supervisors for their guidance, encouragement, and invaluable contributions throughout my master's study. Also, for their patience and support during my illness and allowing me to continue my research. Special thanks to Dr. Liuchen Chang for allowing me to be a part of the Smart Grid Research Lab at UNB. Many thanks to Dr. Tohid Rahimi for his guidance and contribution, without which it could have been very difficult to complete this project.

I am grateful for the continuous support received from my family and friends. Thanks for believing in me, encouraging me, and pushing me all these years towards my goal.

Table of Contents

List of Figures

List of Tables

Abbreviations

APC	Active Power Curtailment
BESS	Battery Energy Storage Systems
DG	Distributed Generator
DVWC	Dynamic Volt-Watt Control
FSC	Fixed Slope Control
MG	Microgrid
OpenDSS	Open-Source Distribution System Simulator
PCC	Point of Common Coupling
PMPP	PV maximum power point
pu	Per Unit
PV	Photovoltaic
SI	Smart Inverter
VSC	Voltage Sensitivity Coefficient
VVC	Volt-Var Control
VWC	Volt-Watt Control

Chapter 1

Introduction

This chapter presents the background and motivation of the research work, followed by research problems and our objectives toward solving that problem.

1.1 Background and Motivation

Penetration of solar photovoltaic (PV) energy into electric power systems has increased rapidly in recent years and continues to increase at a high rate. According to the forecasted data of the International Energy Agency (IEA) shown in Figure 1.1, distributed PV generation will double by 2028 [1] globally. The intermittent nature of the PV generation and the dynamic nature of the electricity demand could result in voltage sag or swell at the point of common coupling (PCC). This may lead to equipment malfunctions or even damage devices connected to the system. Without a proper control strategy, the high penetration of PVs can lead to overvoltages beyond permissible limits, consequently there may be limits on the number of PVs that can be hosted by a feeder.

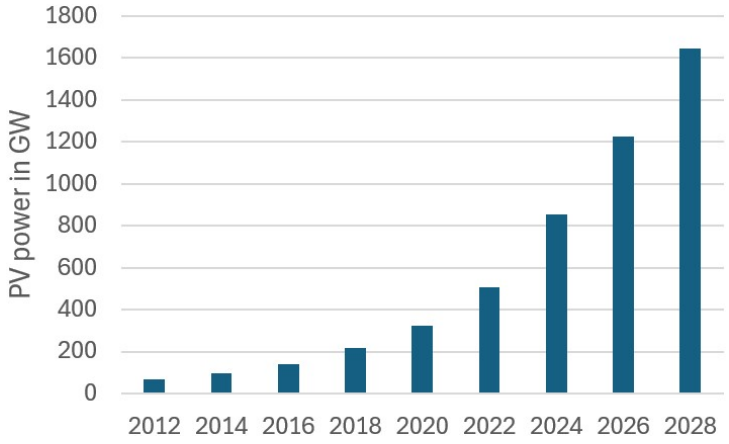

Figure 1.1: Distributed PV generation forecast [1].

Some studies have shown that circuit losses and voltage regulation deteriorate when PV penetration exceeds 30% of the connected load [2]. Dynamic loads such as electric vehicles may introduce an additional voltage drop by as much as 4.5% at the distribution level [3]. The use of traditional system components such as tap changers, and capacitor banks can elevate the voltage level in such conditions. Still, when these dynamic loads are disconnected the system may experience a sudden voltage rise. Smart grid technologies facilitate the implementation of dynamic control strategies which can enable efficient voltage management in such cases of voltage rise and drop [4]. Studies show that control of reactive power from distributed generators (DG), such as wind and PV, can contribute to controlling voltage [2]. Controlling both active and reactive power can improve the robustness of the overall system further and can allow an increase in DG penetration [5], [6].

Control strategies such as volt-watt control (VWC) provide voltage regulation at the PCC by reducing the active power generation of the PV. Whereas the volt-var control (VVC) strategy generates or consumes reactive power depending on the voltage level as a means to provide voltage regulation support. One or both of these methods have been very popular in recent years to regulate the voltage at the distribution level. According to IEEE 1547-2018, smart inverters (SI) are required to supply reactive power during under-voltage conditions and absorb reactive power during over-voltage conditions [7]. However, in systems with a high penetration of PV generation, reactive power support may not be sufficient to provide voltage regulation and may require reduction of real power generation known as active power curtailment (APC). The volt-watt strategy facilitates APC but may

result in unnecessary and/or unfair curtailment if the control parameters are not carefully selected.

1.2 Research Goal

1.2.1 Problem Formulation

A common solution adopted by distribution network operators worldwide to manage reverse power flow from residential rooftop PV involves schemes such as the volt-watt functionality [8]. Also applying fixed limits on household power exports, either in kilowatts or as a percentage of installed PV capacity can ensure power flow meets the local demand only. Despite their widespread use, these schemes can be unfair and overly restrictive to many households [9]. For instance, in typical radial distribution networks, households located farther from substations experience higher voltages during periods of high reverse power flow [10]. This is due to the cumulative voltage rise along the feeder, which results in volt-watt schemes imposing disproportionate levels of curtailment for PVs at those locations. This disparity can lead to notable energy yield reductions for these households, despite similar installed capacities. An example case study is presented in Appendix A where we showed how disparity of curtailment occurs along the line for the PVs having identical generation capacity.

On the other hand, applying a uniform fixed export limit to all households can be seen as a fairer approach, as it removes locational disparities and results in similar levels of active power curtailment [11]. However, these limits are usually determined conservatively, considering worst-case scenarios, such as maximum generation with low demand,

relatively high PV penetrations, and broad regional policies. This conservative approach often leads to unnecessarily penalizing households in areas with low PV penetration or robust networks, thereby reducing their potential energy yield. Additionally, fixed export limits do not account for dynamic network conditions. This can be particularly problematic in regions where network conditions may change over time.

Therefore, there is a clear need for alternative schemes that can more fairly and effectively manage distributed PV systems. These new approaches should consider dynamic network conditions and aim to optimize available network capacity and ensure a more equitable distribution of curtailment while maximizing the energy yield for all households.

1.2.2 Research Objectives

The objective of this thesis is to develop a new control strategy that can not only regulate node voltages but also provide a fairer, more balanced APC while maximizing PV generation. It is clear from the example presented in Appendix A, that changing the SI parameters in volt-watt and volt-var control settings can positively impact the curtailment of active power as well as reactive power generation/absorption of the PV system. Therefore, the investigation of having these parameters dynamically change has research merit with the result that it will facilitate increased PV penetration, fair curtailment, and improved voltage regulation. The research methodology can be summarized as follows:

1. To investigate and analyze the impact of dynamic volt-watt and volt-var control strategies on power distribution networks with high integration of PV systems.

1.1. Review the existing literature on the integration of PV systems into power distribution networks, focusing on volt-watt and volt-var control methods.

1.2. Evaluate the limitations and drawbacks of conventional volt-watt and volt-var control strategies in managing PV system integration issues.

2. To develop and evaluate methods for dynamically adjusting SI parameters to optimize active/reactive power management while maintaining voltage within specified limits.

2.1. Develop a dynamic volt-watt-var control algorithm capable of adjusting voltage parameters in response to changes in PV generation and load conditions.

2.2. Implement and simulate the developed control algorithms using a suitable power system simulation tool to assess their performance under various scenarios.

2.3. Compare the performance of the dynamic control algorithms against conventional fixed-parameter control methods to identify improvements in system performance and fairness.

2.4. Investigate the feasibility of implementing the developed dynamic control algorithms in real-world power distribution networks with PV integration.

Chapter 2

Literature Review

This chapter provides an overview of voltage regulation and control strategies within power distribution systems.

2.1 Voltage Regulating Devices

An increase or decrease in voltage beyond the permissible range at the distribution level can occur due to many reasons. Some of them include low load demand, unbalanced load distribution, lack of voltage regulation devices, capacitive effect, high distributed generation, and reverse power flow [12]. With more and more PV integration into the system, we are looking at situations where a decrease in load demand can significantly increase reverse power flow to the grid and cause overvoltages. Even so, the interest in generating more and more free energy overwhelms the low-voltage distribution system.

Traditional voltage regulation methods, such as off-load tap changers, capacitors, and voltage regulators, have been integral to the design and operation of electrical grids, originally intended to manage one-way power flow. These methods are well-established and have been effective in maintaining voltage stability across the grid [13]. Voltage regulators, in particular, have been shown to mitigate voltage issues even in networks with significant levels of PV penetration [14]. However, a key limitation of voltage regulators is their relatively slow response time compared to more modern technologies such as PV inverters or battery storage systems [15].

The coordinated operation of on-load tap changers and capacitors can significantly enhance the PV hosting capacity of electrical grids. This coordinated approach not only helps manage voltage more effectively but also requires only minor operational adjustments and incurs minimal additional grid costs, as highlighted in [16]. Despite these benefits, it is important to note that most low-voltage networks are connected to off-load tap changers, which inherently offer limited operational flexibility and adaptability to changing grid conditions.

In addition to traditional power electronic interfaces, battery energy storage systems (BESS) has emerged as a promising solution for voltage regulation in distribution networks. Comparative analyses, such as the one presented in [17], have demonstrated that BESS can deliver voltage regulation performance comparable to that of in-line voltage regulators. Moreover, the coordinated control of distributed BESS has been shown to be an effective strategy for managing voltage in distribution networks [18].

While these traditional methods and BESS offer significant advantages, their implementation often incurs recurring and additional costs, particularly for battery units, which can be a barrier to widespread adoption. In this context, our work focuses on leveraging existing SI technologies to enhance voltage regulation. Local voltage control strategies based on volt-watt and volt-var droop control have been extensively studied. These findings underscore the potential of SIs in enhancing voltage regulation and expanding the PV hosting capacity of electrical grids. By focusing on better utilization of

these inverters, we can achieve significant improvements in voltage stability and grid performance without the need for extensive and costly hardware upgrades.

Apart from providing voltage and frequency regulation, SIs have numerous features that enhance the stability, reliability, and efficiency of the power grid. For example, it has communication capabilities, can manage ramp rate, correct power factor, can monitor its own performance and report to operators, and can restart and re-synchronize with the grid after disconnection [19], [20]. It can also provide protection against overvoltage, overcurrent, short-circuit, and overheating. Moreover, it can record data and provide analytics for system optimization and operation. Figure 2.1 represents a simple block diagram showing the features of a SI.

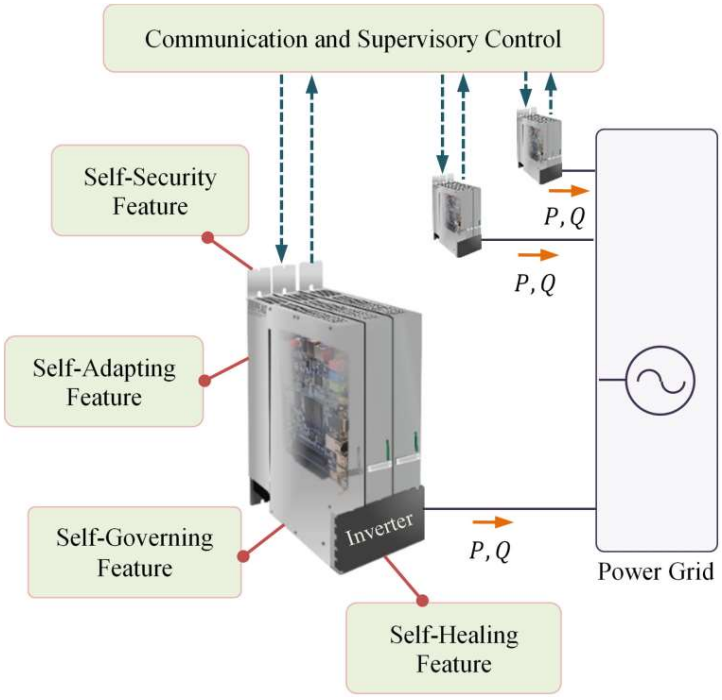

Figure 2.1: SI features beyond active and reactive power delivery [19].

2.2 Voltage Regulation Techniques

Advancements in SI technologies have shifted researchers' focus towards using inverters for voltage regulation support instead of restricting PV integration. The SIs can enable the PV system to generate or absorb reactive power in response to low or high voltage conditions respectively; or reduce the generation of active power when overvoltages occur. One way to do that is to vary the power factor, by controlling the phase difference between generated voltage and current [21].

Droop controllers are also popular for regulating active/reactive power generation. In a droop controller, we can relate two system variables through droop curves, which can control one by changing another. Voltage and frequency may be controlled by controlling active and reactive power as governed by droop curves such as Q-f or P-V curves [6]. Other types of droop curves include Q-V, P-f, V-P, and V-Q as illustrated in Figure 2.2. V-P (VWC) and V-Q (VVC) droop curves, as shown in Figure 2.2, are used to regulate power generation based on node voltage and vice versa. In the context of VVC, DGs inject or absorb reactive power to regulate voltage, thereby increasing the PV hosting capacity of the system by 50-130% depending on the feeder size [22], [23]. When reactive power support is insufficient to maintain the voltage within specified limits, active power generation curtailment may also be needed. VWC enables curtailment of power from the PV as necessary when such cases arise.

In these control strategies, APC is exercised whenever necessary to reduce voltage directly or to allow more var support. APC can significantly increase the penetration of PV energy

often up to three times more than the usual PV hosting capacity of the system [5]. However, it may lead to a larger APC than required, which can be reduced with improved system design. One example is proposed by Alonso et al. [24] where a central controller is employed to coordinate active/reactive power sharing from PV, wind, and BESS to mitigate overvoltage while reducing unnecessary APC.

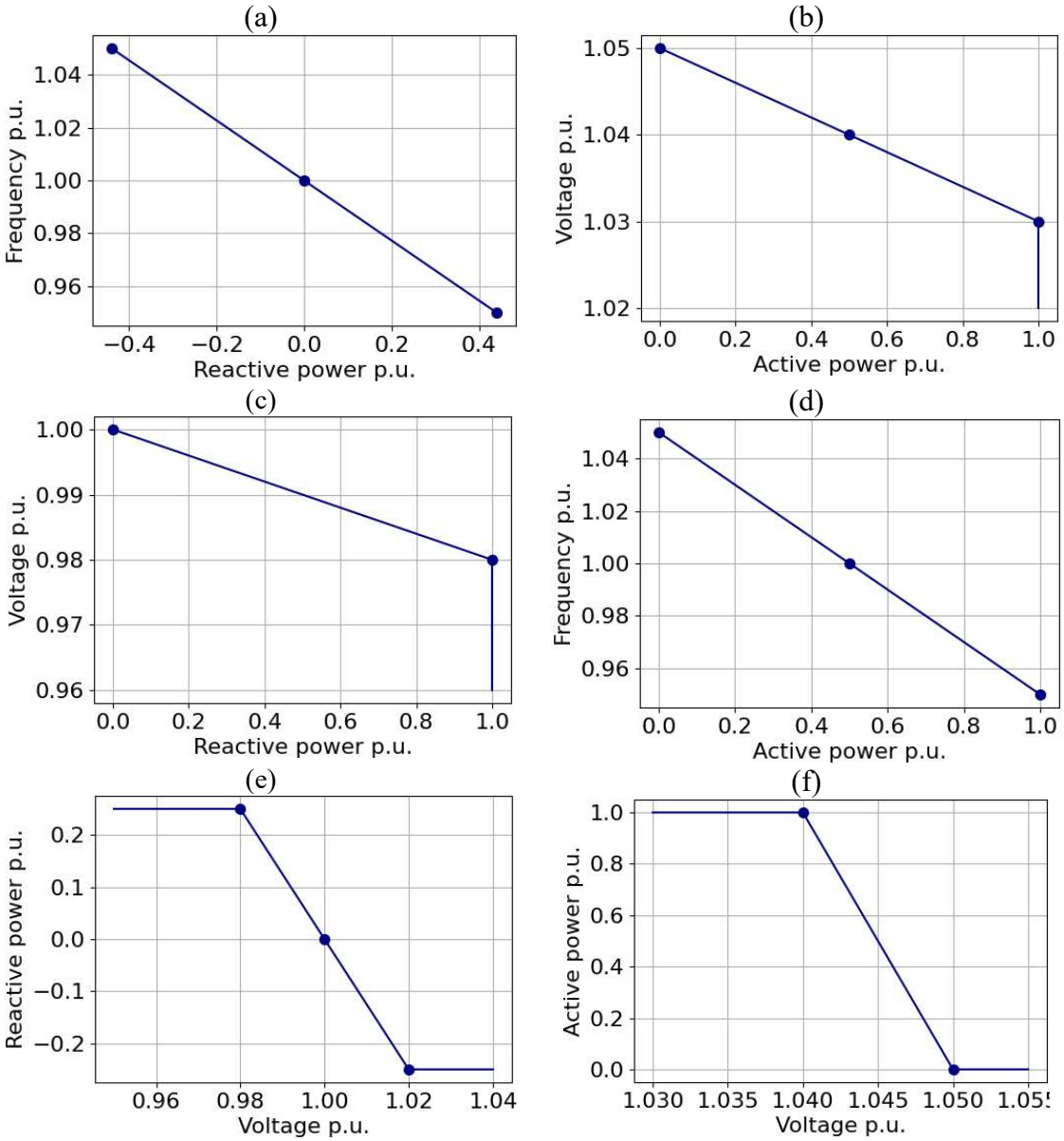

Figure 2.2: Example droop curves (a) Q-f, (b) P-V, (c) Q-V, (d) P-f, (e) V-Q and (f) V-P.

2.3 Centralized vs Distributed Control

2.3.1 Advantages and Disadvantages of Centralized Control

A centralized control strategy, which involves a single control unit managing and optimizing the operation of various devices across the network, can be an effective approach for regulating voltage at the distribution level. It is not constrained by the size of the network, can make informed decisions based on the monitored data, and can optimize DG generation to reduce losses and improve efficiency. Moreover, it can coordinate control between other regulating devices e.g. tap changers, capacitors, regulators, and static var compensators [25]. Inaolaji et al.[26] presented a centralized volt-var-watt control strategy based on fixed SI parameters, providing var support to minimize overvoltage situations and APC when necessary. Lee et al. [27] proposed an optimized VVC where parameters are determined using a genetic algorithm that minimizes voltage deviation, system loss, and peak reactive power. The method is not tested in a larger system with overwhelming PV integration. Olowu et al. [28] proposed a centralized VVC and VWC capable of changing control parameters dynamically based on objective functions that minimize active power loss and voltage deviation. However, their resulting VWC curve curtails PV power to 50-60% for normal operating voltage. A centralized fair curtailment control strategy is proposed by Mohamed Ali et al. [29] that uses voltage sensitivity information to calculate the required APC to regulate voltage. Their proposed method resulted in more total APC than fixed parameter VWC.

Moreover, centralized controllers can prove more costly to implement due to the requirement for monitoring devices and communication infrastructure. In practice, there is

a further requirement for a reliable communication network that is resilient to cyber-attacks, and any communication malfunction.

2.3.2 Advantages of Distributed Control

In contrast, distributed control offers several advantages over centralized control, particularly in terms of scalability, resilience, and responsiveness. Unlike centralized control, where a single control point can become a bottleneck and a potential single point of failure, distributed control distributes decision-making across multiple entities, improving fault tolerance and reducing communication overhead. In distributed systems, control tasks are handled by local controllers that manage specific parts of the system, ensuring that even extended communication failures have little to no impact on local control [30], [31]. Additionally, a decentralized approach enables faster, more adaptive responses, as decisions are made locally at individual nodes, allowing for quicker actions and reduced latency [32]. While distributed systems may be more complex to implement initially, they scale more efficiently and ensure that failures in one part of the system have minimal impact on overall performance. The ability to process data locally also reduces delays and congestion, making distributed control better suited for dynamic, large-scale systems.

Several studies have explored different decentralized strategies for managing voltage and power flow in distribution networks. Joseph et al. [33] introduced a decentralized VVC method aimed at improving voltage stability by minimizing the switching actions of voltage regulatory devices, though it did not include APC support. Collins et al. [34], on

the other hand, presented a distributed control strategy incorporating APC, where the adjustment of the VWC curve is based on the inverter's rated power, but the slope remains fixed. A more dynamic approach to VWC is proposed by Noh et al. [35], who developed a hierarchical scheme that determines SI parameters based on the voltage at the PCC, although var support is not included. Yoshizawa et al. [36] took a broader approach with volt-var-watt control, integrating both var support and APC. Their method dynamically determines droop curve parameters through voltage sensitivity analysis but ultimately settles on fixed parameters without addressing potential fairness issues across the system.

2.4 Fairness in Active Power Curtailment

Fairness in PV power curtailment involves ensuring equitable treatment of various stakeholders and maintaining system reliability while maximizing the benefits of renewable energy sources. As PV systems connected to the grid all contribute to voltage rise, curtailing each system by the same percentage of its capacity can be considered fair because it ensures an equal level of participation in maintaining grid stability. By curtailing power uniformly across all systems, each PV system shares an equal burden relative to its capacity, preventing over-curtailment of smaller systems or under-curtailment of larger ones. This approach maintains balance and fairness while avoiding disproportionate impacts on specific PV installations.

Achieving fairness poses several challenges. It requires grid information, monitoring and communication, and more importantly a dynamic curtailment algorithm. Most of the fairness algorithms in the literature employ a centralized controller that can continuously

acquire system data related to node voltages and PVs active power generations [9], [29]. Even so, it led to an undesirable increase in total curtailed power in these literatures. Gupta et al. [37] presented a centralized system that optimizes power output to improve fairness in curtailment as well as PV owners' income from importing power.

A distributed VWC is proposed by Kashani et al. [38] which dynamically sets SI parameters utilizing voltage sensitivity information to achieve fair APC. They considered VWC curves for some PVs where 100% curtailment occurs at different voltage levels exceeding 1.05 per unit (pu). Such a curve may cause a significant disparity in curtailment across PVs under low-load conditions. Also, their algorithm seems to be model-specific and may not be fair when applied to a large system. Another example is presented by Haque et al. [39] which uses the consensus algorithm to determine SI parameters for volt-watt curves. As the results suggest, failure in communication between feeders will cause tremendous unfairness in APC. Moreover, in both papers, the frequency of updating SI parameters is not clearly specified, which is a significant oversight. Regular updates are essential for adapting to changing network conditions and optimizing performance, but excessive or poorly timed updates can lead to instability, particularly during APC. Frequent adjustments in SI parameters during APC can induce oscillatory behavior, as the system may continuously shift between different states in response to changing inputs, ultimately degrading system stability and performance [36], [40]. Therefore, finding the right balance in update frequency is crucial to avoid such oscillations and ensure effective, stable control of the distribution network.

There is very limited literature that addresses fairness contributions in the context of the volt-var-watt droop control strategy. Moreover, though the voltage sensitivity coefficient (VSC) base algorithm is more efficient in mitigating overvoltage situations, it is yet to offer better fairness in APC [40].

2.5 Dynamic Control Strategy Based on Voltage Sensitivity Coefficient

VSC is the measure of how voltage at a particular node change in response to active/reactive power injections/reduction. These coefficients can be used to configure control algorithms that can improve voltage regulation, system stability, and optimal power flow. A small signal linearized model may be expressed as

$$\Delta V = R\,\Delta P + X\,\Delta Q \quad (1)$$

where, ΔV = voltage deviation at the node in pu

ΔP = changes in PV active power in pu

ΔQ = changes in PV reactive power in pu

R = active power voltage sensitivity coefficient

X = reactive power voltage sensitivity coefficient.

One popular method of calculating VSCs is to find the Jacobian matrix through linear analysis and use its inverse form to obtain R and X [29]. This approach enables a systematic examination of the system's behavior, particularly regarding voltage regulation. Another way is to use system resistance and reactance matrices as R and X respectively which remain constant as long as there is no topological network change [38]. This consistency can simplify calculations and enhance the efficiency of VSC implementation. Additionally,

the Thevenin equivalent method is commonly used to calculate the Thevenin equivalent resistance (R^{th}) and reactance (X^{th}) at the PCC [28]. However, all these methods require a comprehensive understanding of the system's configuration and parameters. As the system evolves, the variability of resistance and reactance can introduce challenges in maintaining accurate and reliable calculations for real-time implementation.

One approach to calculate VSCs is using the perturb and observe method [36]. In this method, voltage deviation is determined by slightly increasing or decreasing active or reactive power, with R and X calculated separately under the assumption that they are relatively constant. Although this method is straightforward, it may introduce small disturbances into the system, depending on the magnitude of the perturbations and the accuracy of the measurements. Depending on the calculation method and the measurement techniques employed, VSC can either represent the influence of a PV system on its connected node or encompass the cumulative effects of all PVs connected to the system at that node. The former approach, adopted by Yoshizawa et al.[36], considers a 25% influence from neighboring PVs; however, this approximation lacks detailed explanation or validation. Conversely, the latter approach is more reasonable for VSC calculation, as demonstrated by Seuss et al. [40], who approximate voltage deviation at any node based on an equal APC applied to all PVs. In this thesis, the latter strategy is employed for VSC calculation, as elaborated in the methodology section.

2.6 Review of Literature and Research Focus

Traditional voltage regulating devices, while effective in certain contexts, have several drawbacks, particularly in modern power systems that face increasing complexity due to the integration of distributed energy resources such as rooftop solar PV. They are slow to respond, have limited control capability, are less flexible to modern grids with dynamic loads, and wear out over time. In comparison, SIs offer quicker response time, data acquisition and communication capability, subject to less wear and tear, and facilitate grid modernization. This research leverages these capabilities to establish a distributed control scheme for regulating distribution system voltages using SIs.

In particular, we focus on developing two VWC algorithms that adjust SI parameters dynamically based on VSCs at PV-connected nodes. The proposed VWC strategy is supported by the reactive power absorption capability of SIs to mitigate overvoltage issues and ensures fairness when APC is required. By using VSCs, we can dynamically select droop curve parameters, eliminating the need for speculative calculations on voltage deviations caused by PV generation changes across the network. Our approach requires minimal communication infrastructure, which is simple to implement. The approach requires no centralized communication, making it a practical solution for real-world applications.

These strategies are validated through simulations on the IEEE 37-bus system under various PV penetration scenarios, demonstrating their effectiveness in managing voltage rise and ensuring equitable APC. A comprehensive comparison with existing methods is

presented in Table 2.1, showcasing the advantages of our proposed approach in addressing modern distribution network challenges.

Table 2.1: Comparison between proposed strategy and some previous work found in the literature.

Ref.	Strategy	Volt-Var	Volt-Watt	System architectures	Fairness consideration	Communication Frequency
[41]	Volt-var-watt parameter selection with stability robustness	Yes	Yes	Distributed	No	Low
[42]	Hierarchical control with multi-objective optimization	Yes	Yes	Centralized	No	High
[43]	Coordinated droop control with genetic algorithm	No	yes	Centralized	No	High
[44]	Master/slave coordination with power-based control	No	Yes	Centralized	No	High
[9]	Multi OPF based volt-watt control	No	Yes	Centralized	Yes	Medium
[24]	Local and coordinated volt-watt and volt-var control	Yes	Yes	Centralized	No	High
[27]	Optimal volt-var control with genetic algorithm	Yes	No	Centralized	Yes	Medium
[38]	VSC based smart inverter volt-watt control	Yes	Yes	Distributed	Yes	Low
[35]	Fixed parameter volt-watt control	No	Yes	Distributed	No	Low
[36]	VSC based volt-var-watt control	Yes	Yes	Distributed	No	Medium
[37]	Fairness-promoting optimization method	Yes	Yes	Centralized	Yes	High
[45]	Fairness-Aware Distributed Energy Coordination	Yes	Yes	Distributed	Yes	Medium
[46]	Model-Free Fair PV Curtailment via Reinforcement Learning	No	Yes	Distributed	Yes	Medium
[47]	Multiphase Smart Inverter Optimization	Yes	Yes	Centralized	Yes	High
[48]	Decentralized Voltage Coordination in Unbalanced Network	Yes	Yes	Distributed	Yes	Low
This thesis	VSC based dynamic volt-var and volt-watt control	Yes	Yes	Distributed	Yes	Low

Chapter 3

Methodology

In this section, we detail the approach used to investigate the impact of VSC on APC within a distribution network. The methodology begins by analyzing an example circuit with three variations of load, illustrating how VSCs are connected to the curtailment sequence. Building on this analysis, two algorithms are developed to improve fairness in APC while mitigating overvoltage situations. To evaluate the fairness of these algorithms, we employ a variance-based fairness measure. Next, we describe the simulation setup, which utilizes open-source distribution system simulator (OpenDSS) for power system modeling and Python for control and data analysis. Finally, we present the design consideration of the distributed communication framework that enables the coordination and control of the PVs connected to the system.

3.1 Example System for Sample Case Study

The primary goal of the decentralized control scheme is to regulate the voltage within permissible limits using dynamic volt-var and/or volt-watt control when there is an increased number of PV units. To demonstrate and evaluate these strategies, we begin with a smaller network as illustrated in Figure 3.1. In this system, the grid voltage is 132 kV, and the distribution side voltage is 6 kV. For all experiments we consider the line impedances to be symmetrical, the transformer connection is delta-wye, and loads are wye-connected and balanced. We have connected PVs to all load buses, except bus 701,

assuming all loads are primarily supported by PV power. The apparent power of each PV is rated equal to 80% of the corresponding load kW. PV maximum power point (PMPP) is set to 90% of the rated KVA to allow maximum var support from each inverter of 44% of KVA.

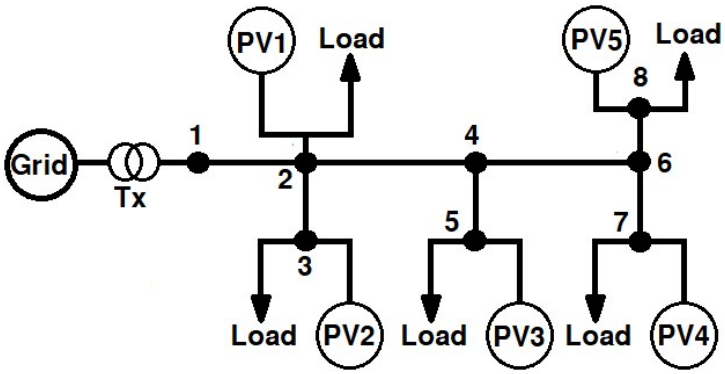

Figure 3.1: Test model for analysis.

The load profiles presented in Table 3.1 represent three distinct cases that were carefully selected to analyze how voltage rise at a particular PV node is related to its VSC. In case 1 we have an identical 420 kW load at each node. In case 2 and case 3, the node loads vary from 210 kW to 840 kW but with the total load constant.

Table 3.1: Different load profile for case studies.

Bus	loads in case 1	loads in case 2	loads in case 3
2	420 kW, 210 kVAR	210 kW, 105 kVAR	840 kW, 420 kVAR
3	420 kW, 210 kVAR	840 kW, 420 kVAR	210 kW, 105 kVAR
5	420 kW, 210 kVAR	420 kW, 210 kVAR	630 kW, 315 kVAR
7	420 kW, 210 kVAR	420 kW, 210 kVAR	210 kW, 105 kVAR
8	420 kW, 210 kVAR	210 kW, 105 kVAR	210 kW, 105 kVAR

3.2 Calculation of Voltage Sensitivity Coefficient

Equation (1) shows that coefficient R is related to deviation in active power only. This thesis addresses the dynamic configuration of the volt-watt curve. Therefore, we only

calculate the coefficient R. To calculate the R of a particular PV node, first, we consider all other node loads and PV generations remain constant, and there is no reactive power generation/absorption. In this case, we can determine the voltage deviation that results by changing the PV power at the selected node only. We can calculate R from equation (3) by increasing the generation from 0% to a small amount or curtailing the power slightly from 100%. The resulting R's for the three cases are listed in Table 3.2. For 'i' number of buses, when $\Delta Q_i = 0 \; \forall \; i$, from equation (1) we get,

$$\Delta V^n = \sum R_i^n \Delta P_i$$

$$= R_1^n \Delta P_1 + R_2^n \Delta P_2 + \cdots + R_n^n \Delta P_n + \cdots + R_i^n \Delta P_i \qquad (2)$$

where R_i^n is sensitivity coefficient of bus 'n' relative to changes in active power at bus 'i' and ΔP_i is active power change at bus 'i'. ΔV^n denotes amount of voltage deviation at bus 'n' in pu.

If $\Delta P_i = 0 \; \forall \; i \neq n$ then from (2) we get,

$$\Delta V^n = R_n^n * P_{cur}^n$$

$$\boldsymbol{R_c^n = \frac{\Delta V^n}{P_{cur}^n}} \qquad (3)$$

where, $P_{cur}^n = \Delta P_n$ = amount of APC for PV connected at bus 'n' in pu

$R_c^n = R_n^n$ = sensitivity coefficient of bus 'n'.

Voltage deviation at bus 'n' can be calculated from,

$$\Delta V^n = V_t^n - V_{t+1}^n \qquad (4)$$

where, V_t^n and V_{t+1}^n denotes pu voltage at bus 'n' before and after APC respectively.

Table 3.2: VSCs obtained using equation (3) for different cases.

PV Bus (n)	Case 1		Case 2		Case 3	
	PV kVA	R_c^n	PV kVA	R_c^n	PV kVA	R_c^n
2	336	.00249	168	0.00121	672	0.00499
3	336	.00327	672	0.00653	168	0.00167
5	336	.00421	336	0.00425	504	0.00633
7	336	.00423	336	0.00426	168	0.00215
8	336	.00452	168	0.00227	168	0.0023

Because of the differences in loads, VSC may also vary across nodes. The load at bus 3 changes in every case, as well as its VSC. But if we look at VSC values for bus 5 and bus 7 in case 1 and case 2, and bus 8 in case 2 and case 3, there is less change in VSC values as the load value is the same. This analysis suggests that VSCs are relatively stable, primarily influenced by the kVA rating of the PV systems rather than variations in load or PV generation. However, a significant limitation of these VSCs is that they do not account for the influence of neighboring PVs. Consequently, it becomes challenging to assess the cumulative effect of all PV units' generation at a specific node based solely on these VSCs.

To account for the influence of neighboring PVs we follow a different method for calculating VSCs. Unlike the previous method, which assumes that other PVs remain constant, this approach involves simultaneously curtailing all PVs by 2-3% from their maximum capacity. This method captures the collective impact of curtailing all PVs, providing a more accurate representation of their influence, especially during periods of curtailment. The calculation of VSCs follows equations (4) and (6), and the resulting VSCs are listed in Table 3.3. We observe from the table that the VSCs are no longer constant and change with system topology. As all the PVs are curtailed in equal amounts we can write,

$$\Delta P_1 = \Delta P_2 = \Delta P_3 = \cdots = \Delta P_i = \Delta P.$$

Therefore, equation (2) can be rewritten as:

$$\Delta V^n = (R_1^n + R_2^n + \cdots + R_n^n + \cdots + R_i^n) * \Delta P.$$

Or $$\Delta V^n = R_{cof}^n * \Delta P \quad (5)$$

$$\boldsymbol{R_{cof}^n = \frac{\Delta V^n}{P_{cur}^n}} \quad (6)$$

where, R_{cof}^n is the sensitivity coefficient of node 'n' due to simultaneous APC of 'i' number of PVs.

Table 3.3: VSCs obtained using equation (6) for different cases.

PV Bus (n)	Case 1		Case 2		Case 3	
	PV kVA	R_{cof}^n	PV kVA	R_{cof}^n	PV kVA	R_{cof}^n
2	336	0.01131	168	0.01133	672	0.01134
3	336	0.01206	672	0.01283	168	0.01175
5	336	0.01441	336	0.01404	504	0.01463
7	336	0.01475	336	0.01427	168	0.01376
8	336	0.01502	168	0.01405	168	0.01391

3.3 Relating Voltage Sensitivity Coefficients with Active Power Curtailment

Applying VWC with a constant slope as shown in Figure 2.2 (f), which we named the fixed slope control (FSC) technique, PVs will start curtailing active power when node voltage exceeds the lower control voltage range, v_{cl}=1.04 pu and comes to a complete shutdown at the upper control voltage range, v_{ch}=1.05pu. We need to understand which bus voltage enters the control region first to understand the variation in their curtailed power. Such as, in case 1 when the connected load is reduced to 20% of its rating, we can see node voltages cross the 1.04 pu range as shown in Figure 3.2 (a) with no control applied. Figure 3.3 (a) shows the voltage profile for the FSC that results in APC which is shown in Figure 3.3 (b).

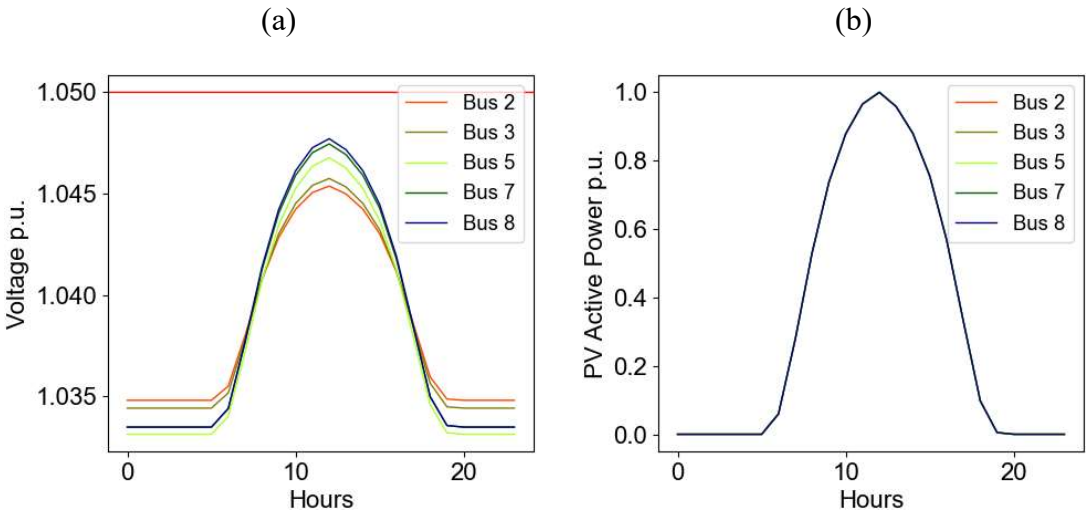

Figure 3.2: (a) Voltage profile and (b) PV profile with no control applied.

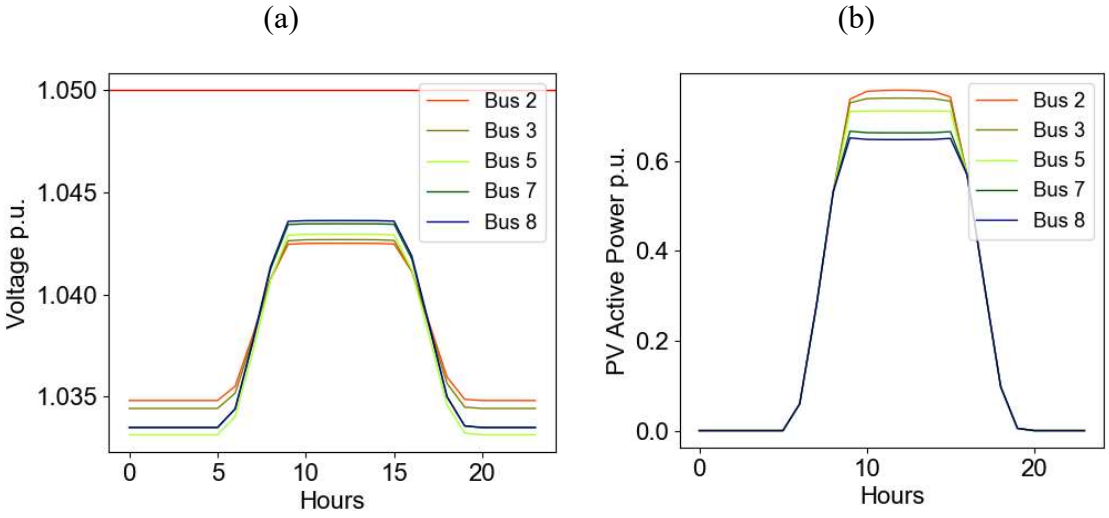

Figure 3.3: (a) Voltage profile and (b) PV profile with FSC applied.

We can see in Figure 3.2 (a) that bus 8 voltage is higher than the others and bus 2 is the lowest. This resulted in more APC for PV at bus 8 and least for PV at bus 2 as can be seen in Figure 3.3 (b). We ran another experimental simulation to observe the sequence of PVs that starts curtailing first. We ran the simulation with all PVs generating at their maximum capacity and gradually reduced the connected load from 100% to 1%. The resulting PV generation profile is shown in Figure 3.4 (a).

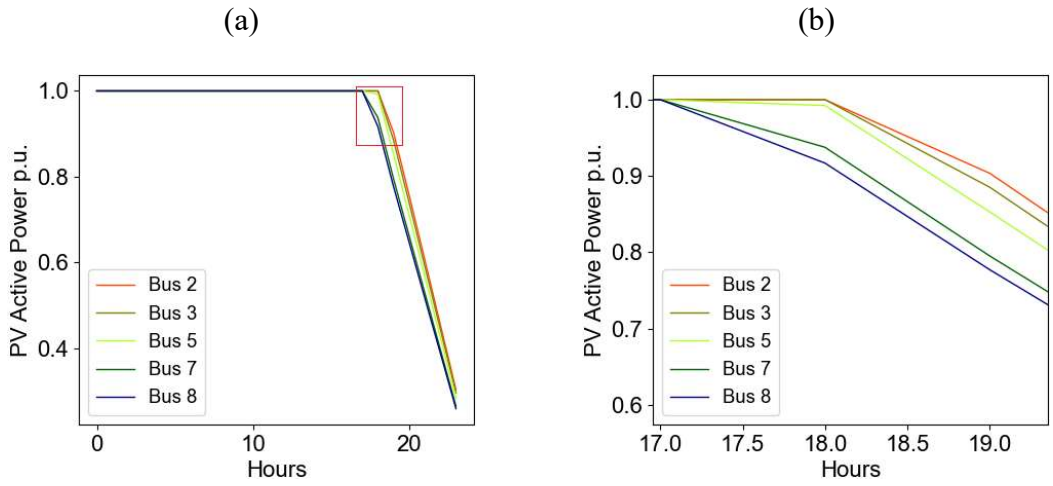

Figure 3.4: (a) PV profile which is (b) zoomed around the red box to check curtailment sequence for case 1.

We observe from Figure 3.4 (b) that PV at bus 8 starts APC, as its voltage reaches control voltage 1.04 pu first. Then bus 7, bus 5, bus 4 and lastly bus 2. If we compare the sequence with VSCs calculated in Table 3.2 and Table 3.3, we observe the curtailment sequence matches the sequence of VSC values. This implies buses with higher values of VSC are more likely to enter the control region first. We ran the same simulation for case 2 and case 3, and the results can be seen in Figures 3.5 (a) and 3.5 (b).

The results show for case 2, PV at bus 7 starts curtailing first and PV at bus 2 last. In case 3, PV at bus 8 starts curtailing first and PV at bus 2 last. Now if we compare all three cases it is evident that the curtailment sequence matches Table 3.3 and not Table 3.2. The detailed comparison is given in Table 3.4 where the bus sequence is given for values of R_c and R_{cof} in descending order, and the sequence of which bus starts APC first.

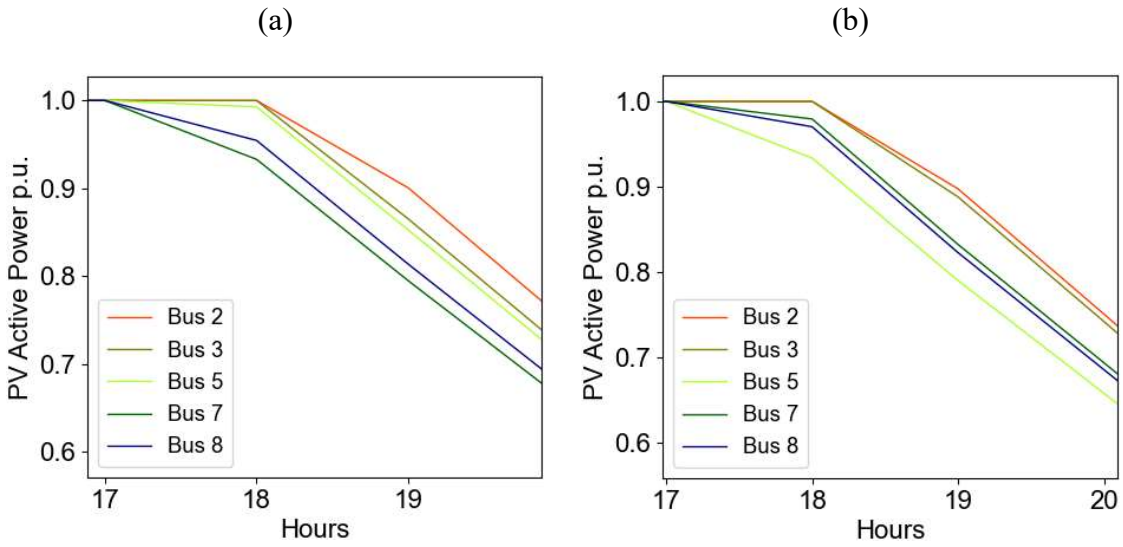

Figure 3.5: Zoomed in view of curtailment sequence for (a) case 2 and (b) case 3.

Table 3.4: Sequence of buses according to their VSCs (descending order) and PV bus that causes APC first.

Case 1				Case 2				Case 3		
R_c	R_{cof}	APC		R_c	R_{cof}	APC		R_c	R_{cof}	APC
8	8	8		3	7	7		5	5	5
7	7	7		7	8	8		2	8	8
5	5	5		5	5	5		8	7	7
3	3	3		8	3	3		7	3	3
2	2	2		2	2	2		3	2	2

From the above analysis, we conclude that whichever bus has the higher value of R_{cof} (VSC for simultaneous curtailment), is more likely to enter the control region first, and start APC. So slowing down the curtailment for PV with higher VSC and increasing the APC rate for PV with lower VSC might give us better fairness, decreasing the disparity in curtailed power.

3.4 Proposed Algorithm

In this study, volt-watt curves with a lower control voltage range v_{cl}=1.04 pu and higher control voltage range v_{ch}=1.05 pu were selected, within which the shape of the curve is modified to provide various slopes. This approach is adopted to ensure a more equitable distribution of APC across multiple PVs. By using these curves, the rate of power reduction is made to be more gradual as VSC increases.

Some studies have proposed shifting the volt-watt control range differently for individual PVs to optimize overall network performance [38]. While this method can provide certain localized benefits, it risks causing imbalances in PV generation across the network. Specifically, PVs with an upper control voltage range lower than v_{ch} may experience shutdowns more quickly, reducing their generation output to zero while other PVs with a control range higher than v_{ch} continue to generate power. This can lead to a scenario where a subset of PVs is fully curtailed while others are not, potentially causing issues related to fairness and efficiency in energy distribution. By maintaining a uniform control range across all PVs, this approach seeks to achieve a more balanced and fair curtailment process, as well as ensure PV inverters enter the shut-down area concurrently. This strategy aims to prevent the premature shutdown of some PVs, thereby maximizing overall PV generation while still adhering to voltage stability requirements.

In this thesis, we propose two distinct dynamic volt-watt control (DVWC) algorithms to improve fairness in curtailment. Both these algorithms are designed to slow down the curtailment for the PVs with higher VSCs and increase the curtailment for PVs with smaller

VSCs. The first algorithm is based on a volt-watt profile that is quadratic and the second algorithm is a hybrid one following two different slopes at different voltage levels. For both methods, we made sure that each .0025 pu voltage deviation resulted $APC \leq 50\%$, as it may cause unexpected jumps in power resulting in the oscillation of voltage [40].

3.4.1 Quadratic Equation Based Dynamic Volt-Watt Control (DVWC_1)

For nodes with higher VSCs, the quadratic profile is designed to decrease the slope of the volt-watt curve. This gentler slope ensures that these nodes curtail their power output more gradually as voltage increases, preventing excessive curtailment for higher VSC PVs. Conversely, for nodes with smaller VSCs, the quadratic profile has a larger slope of the volt-watt curve. This steeper slope means that PVs at nodes with lower VSCs curtail their power output more rapidly as voltage rises. The design steps for this algorithm are explained below.

Step 1: We can express equation (5) as:

$$\Delta V = R_{cof}\, \Delta P \qquad (7).$$

Step 2: We calculate the maximum voltage deviation that can be achieved by curtailing the PV power 100% from:

$$\Delta V_{max}^{PV} = R_{cof}\, \Delta P_{max} = R_{cof} \qquad (\text{as } \Delta P_{max} = 1 \text{ pu}) \qquad (8).$$

Step 3: The parabolic curtailment profile may be described by:

$$P = av^2 + bv + c \qquad (9).$$

Step 4: The parameters, a, b and c, may be tuned for a specific node by imposing the following conditions:

$$P_o = av_{cl}^2 + b\,v_{cl} + c \quad (10)$$

$$0 = av_{ch}^2 + b\,v_{ch} + c \quad (11)$$

$$Slope = 2av_{cl} + b \quad (12)$$

$$= \cot(\alpha) = -\frac{1}{\Delta V_{max}^P} = -\frac{1}{R_{cof}} \quad (13).$$

Equation (10) forces the quadratic profile to intersect P = P_o = 1 at $v = v_{cl}$. Equation (11) forces the profile to intersect P = 0 at $v = v_{ch}$. Equation (12) and (13) forces the slope of the quadratic profile at $v = v_{cl}$ to $-1/R_{cof}$. Solving equations (10-13) for bus 8 with v_{cl}=1.04, v_{ch} = 1.05, and R_{cof} = 0.01502 results in the quadratic profile shown in Figure 3.6.

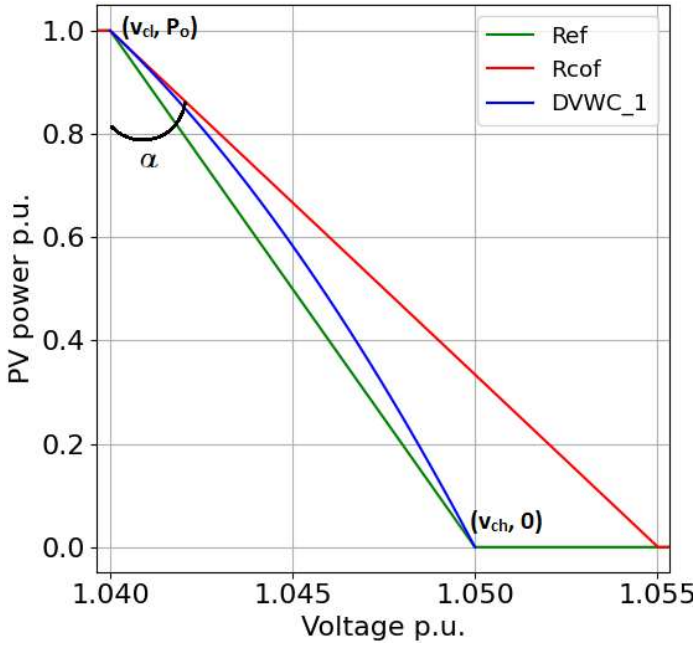

Figure 3.6: DVWC_1 for PV at bus 8.

We can use this curve as our DVWC_1 for SI control. But to configure the control curve in Open-DSS we need to know per unit active power for each selected per unit voltage

point, meaning values for the x-axis and y-axis. Therefore, we solved equations (10-13) in terms of the slope which are given as:

$$a = -100 * slope - 10000 \quad (14)$$

$$b = 209 * slope + 20800 \quad (15)$$

$$c = -109.2 * slope - 10815 \quad (16)$$

$$p = a * v^2 + b * v + c \quad (17).$$

We solve 'p' for the voltage points v = 1.04 - 1.05 pu using equation (17). We chose voltage points .0025 pu apart, so the x-axis and y-axis values to set the volt-watt curve for PV at bus 8 become:

x-axis = (0, 1.04, 1.0425, 1.045, 1.0475, 1.05, 1.1)

y-axis = (1, 1, 0.81267, 0.58356, 0.31267, 0, 0).

3.4.2 Hybrid Sensitivity-Based Dynamic Volt-Watt Control (DVWC_2)

In this algorithm, the first part of the control strategy adjusts the volt-watt curve based on VSCs. This segment of the curve dynamically adapts the VSCs making the initial curtailment follow a slope M_{cof} similar as shown in Figure 3.7. After the voltage reaches 1.045 pu, the control strategy shifts to a fixed slope curve M_{max} (from 1.045 to 1.05 pu). The calculations are as follows:

Step 1: Initialize the starting and end point of the slopes M_{cof} and M_{max}:

$$x_1, y_1 = v_{cl}, 1 \qquad x_2, y_2 = v_{cl} + R_{cof}, 0$$

$$x_3, y_3 = 1.045, 1 \qquad x_4, y_4 = v_{ch}, 0.$$

Step 2: Draw the slopes M_{cof} and $M_{max:}$ using equations:

$$M_{cof} = \frac{y_2 - y_1}{x_2 - x_1} \quad (18).$$

$$M_{max} = \frac{y_4 - y_3}{x_4 - x_3} \quad (19).$$

Step 3: Find the y-intercept of the line with slope M_{cof} and M_{max} from:

$$c_1 = y_1 - M_{cof} * x_1 \quad (20)$$

$$c_2 = y_3 - M_{max} * x_3 \quad (21).$$

Step 4: Find the x and y coordinate of the intersection point of the two lines from:

$$x_{intersect} = \frac{c_2 - c_1}{M_{cof} - M_{max}} \quad (22)$$

$$y_{intersect} = M_{cof} * x_{intersect} + c_1 \quad (23).$$

Figure 3.7 shows the resulting curves for PV at bus 8. The x-axis and y-axis values to setup the volt-watt curve for PV at bus 8 are:

x-axis = (0, 1.04, 1.0475, 1.05, 1.1)

y-axis = (1, 1, 0.5009, 0, 0).

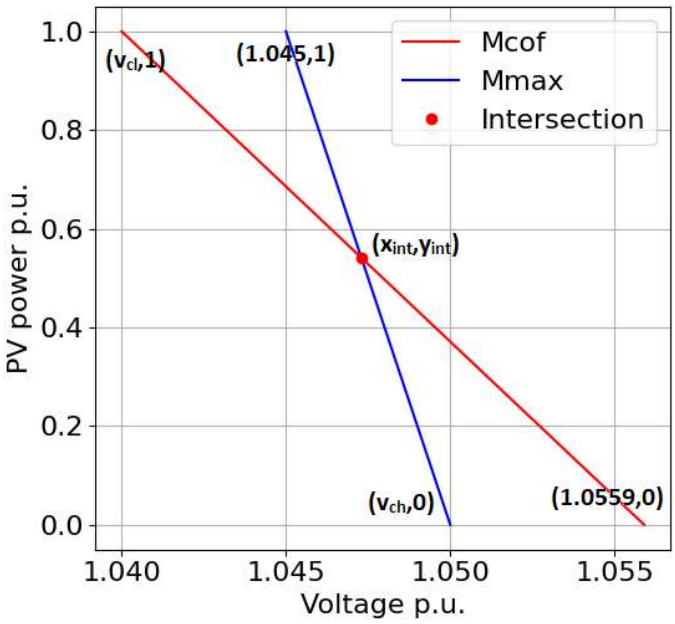

Figure 3.7: Finding the intersection point for lines with slope M_{cof} and M_{max}.

Figure 3.8 shows DVWC_2 curves for all PVs for case 1. In this method, we could not realize any curve for $R_{cof} < .01$. So, for any VSCs less than .01, we kept the curve like the FSC method.

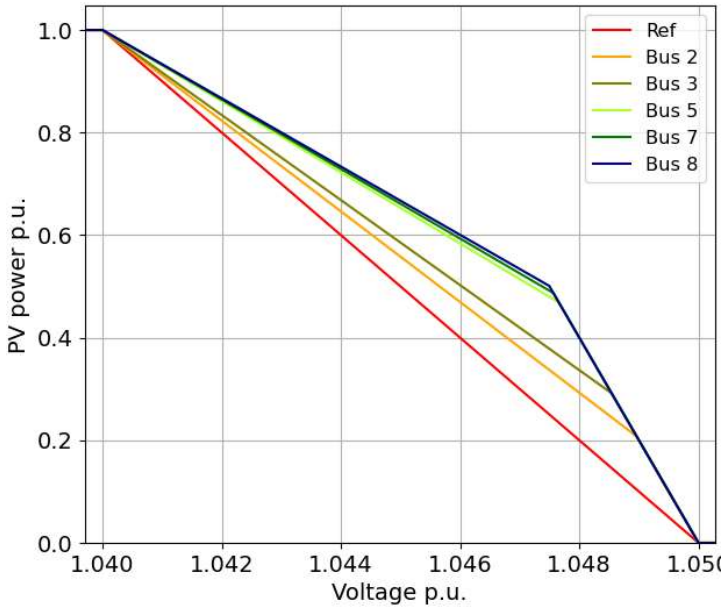

Figure 3.8: DVWC_2 curve for all PVs.

3.5 Variance of Active Power Curtailment

In the context of active power curtailment in power systems, variance refers to the statistical measure that quantifies the dispersion or spread of the active power curtailment values around their mean (average) value over a given period. It indicates how much the curtailment levels deviate from the average curtailment, providing insight into the consistency or variability of power reduction across the system. Mathematically, variance is calculated as the average of the squared differences between each curtailment value and the mean curtailment value. A higher variance suggests greater inconsistency, meaning that some generation units or time periods experience larger differences in the level of

curtailment compared to others, while a lower variance tends to more uniform curtailment across the system. We calculate the variance in the case of FSC and DVWC methods to assess the performance of our algorithm in achieving fairness. The equation is,

$$S^2 = \frac{1}{N} \sum_{i=1}^{N} (x_i - \bar{x})^2 * 100 \qquad (24)$$

where, S is the variance, N denotes the number of PVs, x_i denotes PV curtailed power at bus 'i', and $\bar{x}$ denotes the mean curtailed power. As we are showing PV power as pu which also resembles percentage power, the variance is shown as a percentage in this thesis.

3.6 Simulation Setup

The OpenDSS is the main simulation platform used to model the behavior of the grid. It is a free software developed and distributed by the Electric Power Research Institute (EPRI). We used Python as a supporting tool for data collection, processing, analysis, and plotting.

All of the system information for the grid, transformers, lines, and loads is collected from the OpenDSS repository. The PV unit is designed according to the PV system and inverter control model explained in the reference study [49], [50]. Figure 3.9 shows a block diagram of the PV model. The PV model can follow a pre-specified daily PV profile with actual generation data or data represented in pu. The model also accepts inputs for irradiance, temperature, and efficiency of PV power, and OpenDSS generates the corresponding PV profile itself. In this thesis, we used PV profile data in pu saved in CSV files.

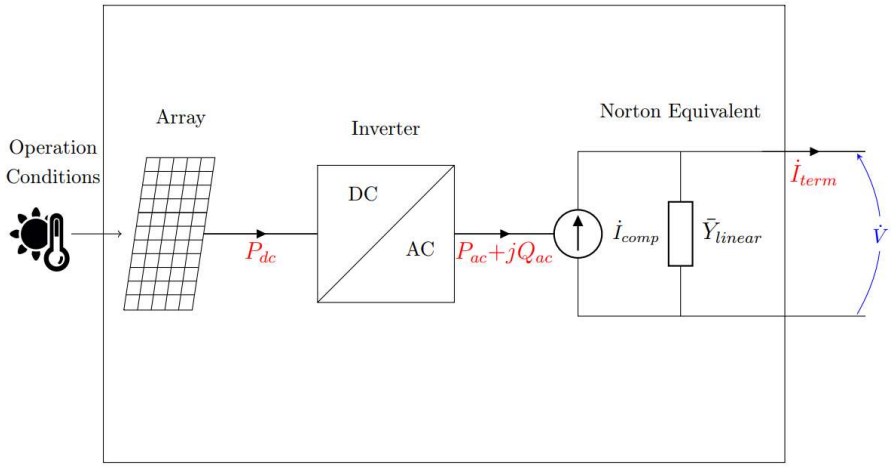

Figure 3.9: Block diagram of PV system model [49].

3.7 Communication Infrastructure

We assumed the SIs to be capable of communicating with a local controller in a form like a microgrid (MG). The MG has knowledge of the system e.g. maximum load demand at a bus node, rating of the PVs, cable size and lengths, network topology, geometry, and distance of the bus node necessary for running static load flows. If the system is large like the IEEE 37-bus or IEEE 123-bus system, it can be divided into several MGs that communicate with each other and share load and PV data. Figure 3.10 represents the IEEE 37-bus system sectionalized into three MGs which we considered for our experiments. This has many advantages such as control complexity reduction, lower communication bandwidth, and tolerance of communication failure where failure in one MG doesn't affect the others [51].

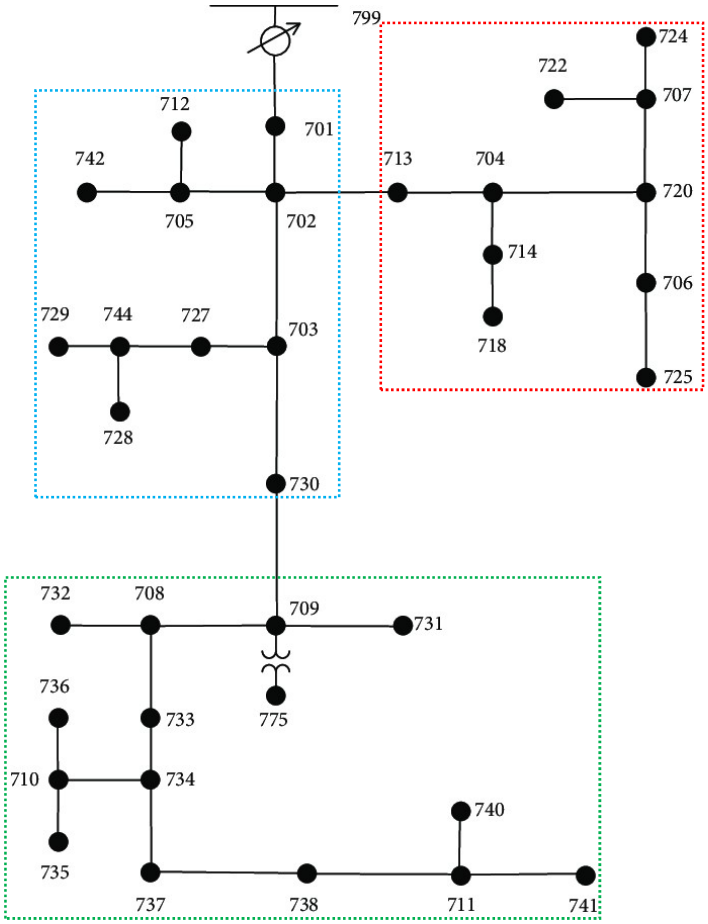

Figure 3.10: IEEE 37-bus divided into three MGs.

Chapter 4

Results

In this chapter, we explore the application of our algorithms to manage PV power in our example circuit, with three distinct load data variations as presented before. This initial step provides a foundational understanding before scaling up to the IEEE 37-bus system, where the algorithms are tested using real-world data with varying time resolutions ranging from 1-hour to 1-minute intervals over a 24-hour period. Next, we simulate scenarios where PVs intermittently switch on and off, to assess the robustness and effectiveness of the proposed methods in dynamic conditions. These experiments demonstrate the algorithms' capability to regulate system voltage and improve fairness under varying load and generation conditions.

4.1 Example Case Study

The configuration of case 1, case 2, and case 3 is described already in Table 3.1 and corresponding VSCs in Table 3.3. As we are demonstrating the fairness of APC, we didn't consider var support for example cases. We reduced the load to an extent that causes voltages to reach the control region for APC to occur. With no control, we have the voltage profile and PV generations as shown in Figure 4.1 for load reduced to 25%. All with PV generation at 100%, the node voltage exceeds the limit of 1.04 pu. By applying FSC, DVWC_1, and DVWC_2 we obtain the voltage profile shown in Figure 4.2 (a), 4.3 (a), and 4.4 (a) respectively.

(a) (b)

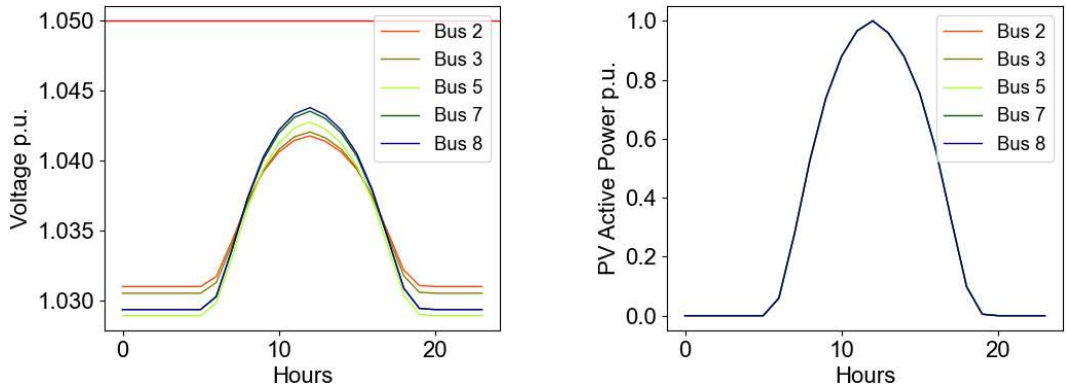

Figure 4.1: (a) Voltage profile and (b) PV profile with no control applied for 25% load.

(a) (b)

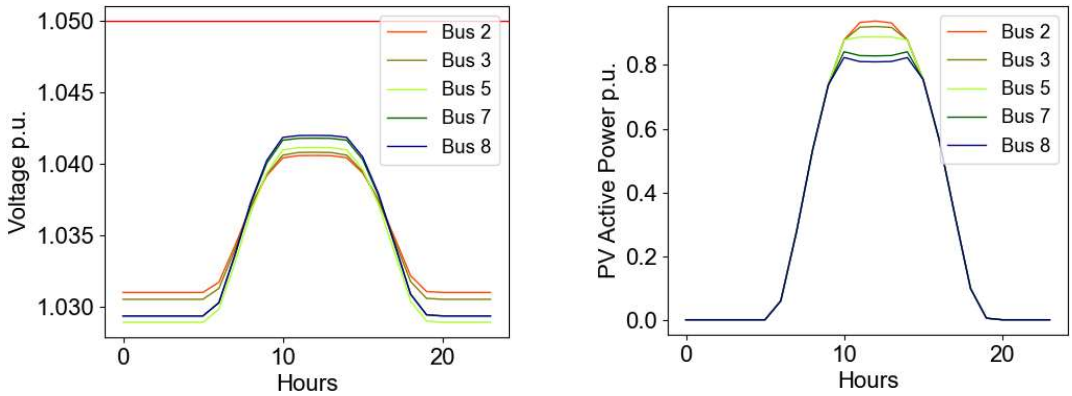

Figure 4.2: (a) Voltage profile and (b) PV profile with FSC applied for 25% load.

(a) (b)

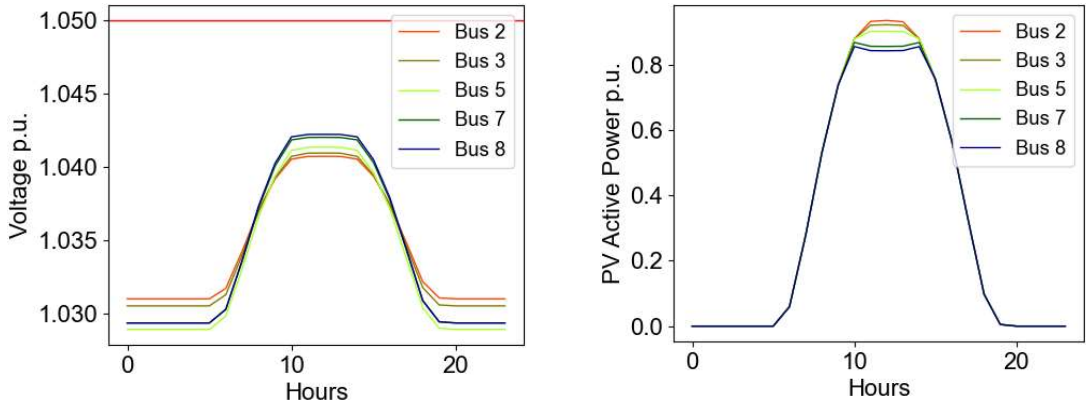

Figure 4.3: (a) Voltage profile and (b) PV profile with DVWC_1 applied for 25% load.

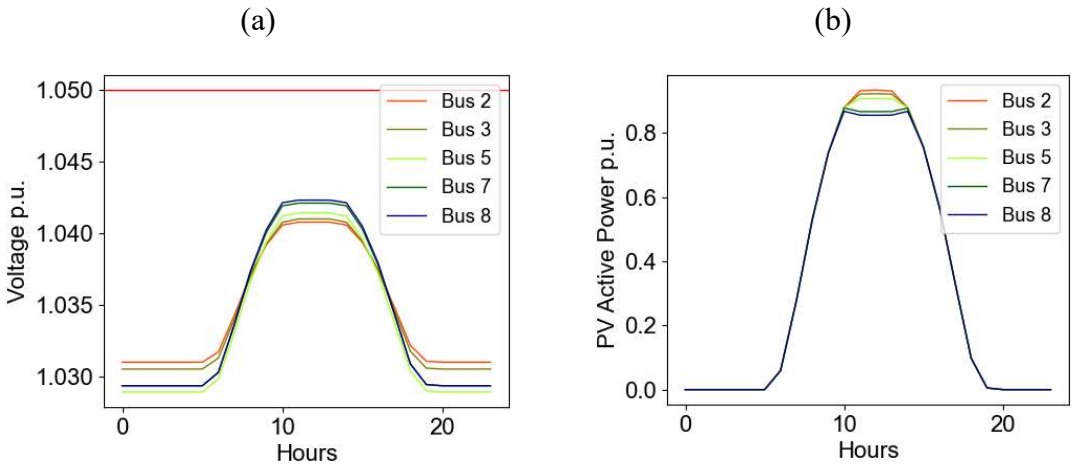

Figure 4.4: (a) Voltage profile and (b) PV profile with DVWC_2 applied for 25% load.

The active power generations for FSC, DVWC_1, and DVWC_2 are shown in Figure 4.2 (b), 4.3 (b), and 4.4 (b) respectively. Looking at the range of APC we can clearly see DVWC_1 offers better fairness than FSC, while DVWC_2 offers slightly more than DVWC_1. The variance with FSC, DVWC_1, and DVWC_2 is shown in Figure 4.5 (a), (b), and (c) respectively. It can be seen that the variance value for DVWC_1 is .17 which is almost half the value with FSC at .33. While DVWC_2 with .12 achieves almost three times reduction in variance which is an indicator of fairness improvement.

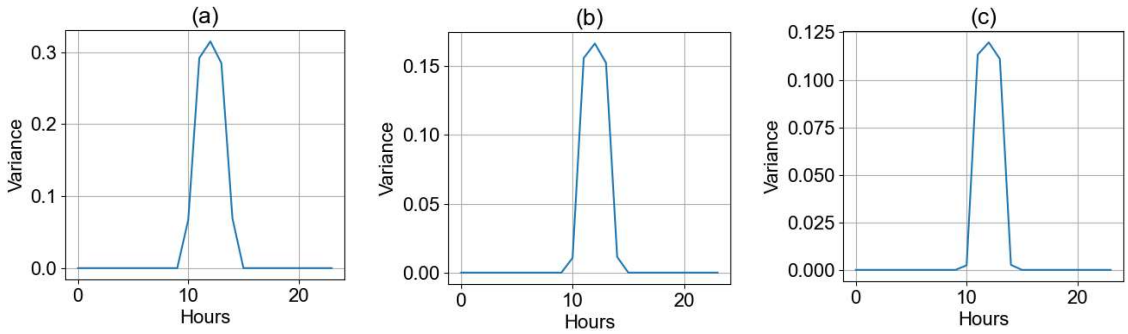

Figure 4.5: Variance with (a) FSC, (b) DVWC_1 and (c) DVWC_2 applied for 25% load.

Next, we reduced the loads to 15% to check how the methods work under lower load. For simplicity, we only included plots related to APC for the three algorithms and variance. We can see comparing Figure 4.6 (a), (b), and (c) that both the DVWC algorithms allow more total PV generation. The variance plots in Figure 4.7 show the reduction of variance by almost four times than FSC for both DVWC techniques which show better fairness is achieved.

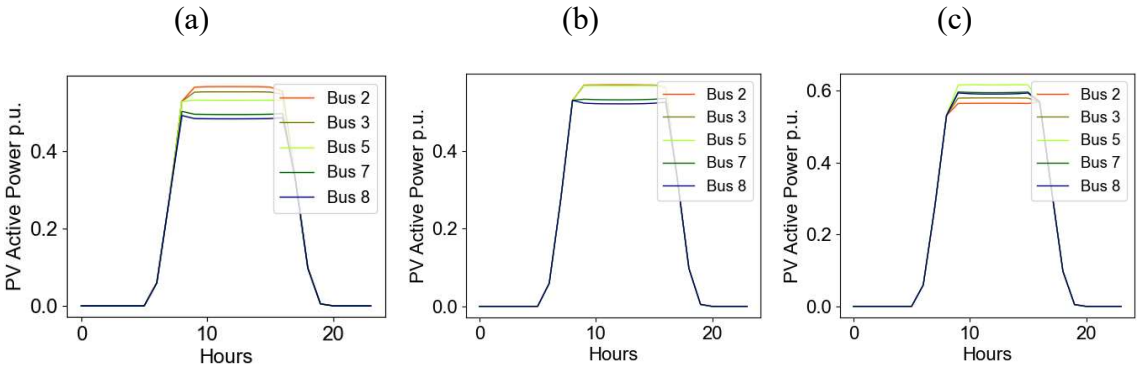

Figure 4.6: PV generation in case 1 with (a) FSC, (b) DVWC_1 and (c) DVWC_2 applied for 15% load.

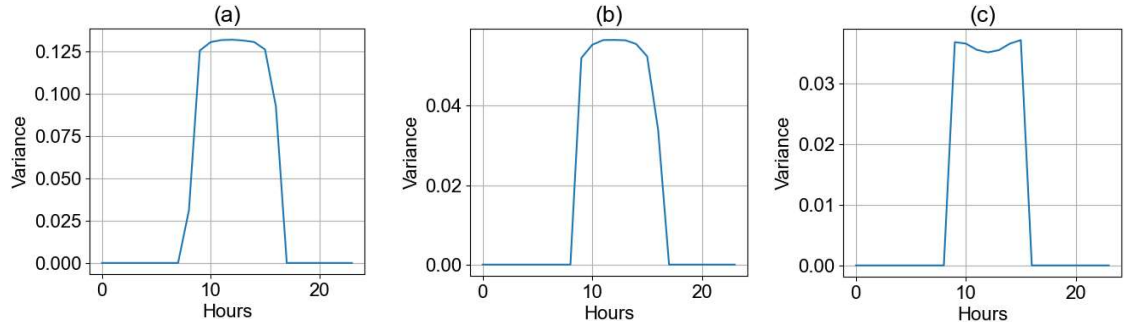

Figure 4.7: Variance in case 1 with (a) FSC, (b) DVWC_1 and (c) DVWC_2 applied for 15% load.

The variance results when the load is reduced to 15% for case 2 is shown in Figure 4.8 and for case 3 in Figure 4.9. The results indicate similar results as case 1, reducing the variance and improving the fairness.

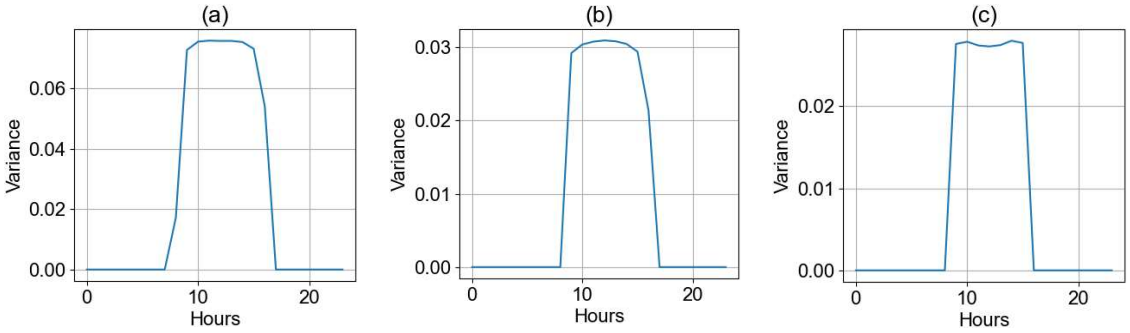

Figure 4.8: Variance in case 2 with (a) FSC, (b) DVWC_1 and (c) DVWC_2 applied for 15% load.

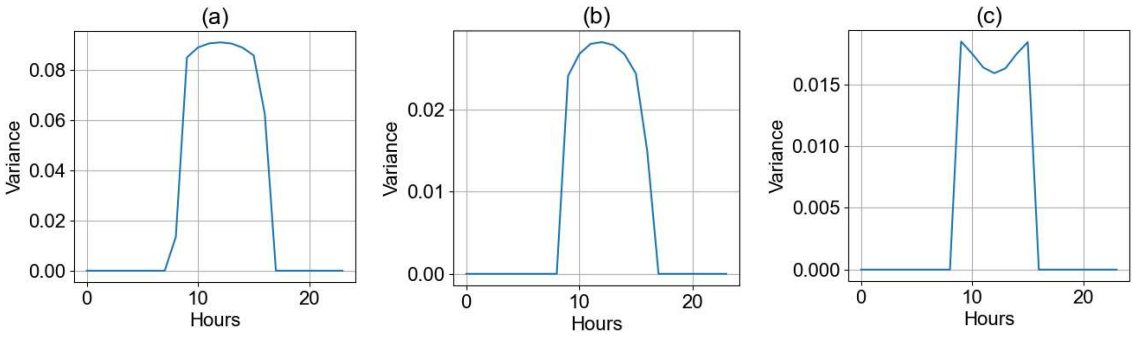

Figure 4.9: Variance in case 3 with (a) FSC, (b) DVWC_1 and (c) DVWC_2 applied for 15% load.

4.1.1 Summary of Example Case Studies

From the analysis of the results provided above we can clearly see both the DVWC methods provide more fairness in APC to minimize overvoltage situations. In case 1, bus 2 has the lowest VSC and bus 8 highest. As a result for FSC, PV at bus 2 curtailed the least, and at bus 8 curtailed most. Though bus 2 remained the lowest for all cases, a similar phenomenon was observed for bus 7 and bus 5 in case 2 and case 3 respectively having the highest VSC and APC. In all cases having a slower rate of APC allowed more PV generation for higher VSC PVs and improved fairness. The variance results also show both

DVWC techniques capability to improve fairness, though DVWC_2 performed better than DVWC_1 in most cases.

4.2 IEEE 37-bus Case Study

We chose the IEEE 37-bus network to evaluate the performance of our algorithm in achieving fairness in APC. This system is readily available in the Open-DSS repository, but it is presented as an unbalanced system. For our experiment, we modified its configuration to convert it into a balanced three-phase system, with symmetrical wire data and balanced three-phase loads. The one-line diagram of this feeder is already shown in Figure 3.10. In this system, the grid voltage is 230 kV, and the distribution side voltage is 4.8 kV. We considered the transformer connection to be delta-wye, and loads are wye-connected. We have connected PVs to all load buses except bus 701, assuming all the loads are primarily supported by PV power. All the PV's apparent power (KVA) are rated equal to 90% of load kW connected to respective buses. PMPP is set to 90% of the rated KVA to allow maximum var support for each inverter to 44% of KVA.

Unlike our example cases, we considered var support for this case study. SIs will provide reactive power support first in response to overvoltage situations. Control action is set such that when node voltage reaches 1.03 pu, PV starts absorbing reactive power to reduce voltage. The max var support is set to 25% and it reaches max at 1.04 pu voltage at each node. 1.04-1.05 pu of voltage is the parameter selected when PVs start APC if var support is not adequate for voltage reduction. The sensitivity coefficients are listed in Table 4.1 for the PV connected nodes only.

Table 4.1: VSC for all PV nodes in IEEE 37-bus system.

Bus	kVA	kW	R_{cof}
712	76.5	68.85	0.01651
713	76.5	68.85	0.01689
714	34.2	30.78	0.01901
718	76.5	68.85	0.01962
720	76.5	68.85	0.02108
722	144.9	130.41	0.02388
724	37.8	34.02	0.02403
725	37.8	34.02	0.02144
727	37.8	34.02	0.02062
728	113.4	102.06	0.02144
729	37.8	34.02	0.02125
730	76.5	68.85	0.0241
731	76.5	68.85	0.02578
732	37.8	34.02	0.02743
733	76.5	68.85	0.02897
734	37.8	34.02	0.0316
735	76.5	68.85	0.03272
736	37.8	34.02	0.03323
737	126	113.4	0.0337
738	113.4	102.06	0.03456
740	76.5	68.85	0.03523
741	37.8	34.02	0.03511
742	83.7	75.33	0.01665
744	37.8	34.02	0.02108

For all purposes, until there is a change in system configuration, meaning no PV is added or removed from the system, these VSCs will be used to configure volt-watt curves of SIs. While calculating these VSCs, we considered the load to be 70% of the rated value. Though load change has little effect on the coefficients and doesn't change the order of highest and lowest VSC, we are rather interested in getting the coefficients considering 70% as the base load. The resulting control curves for DVWC_1 and DVWC_2 for bus 712, bus 730, and bus 740 are shown in Figure 4.10 and Figure 4.11 respectively.

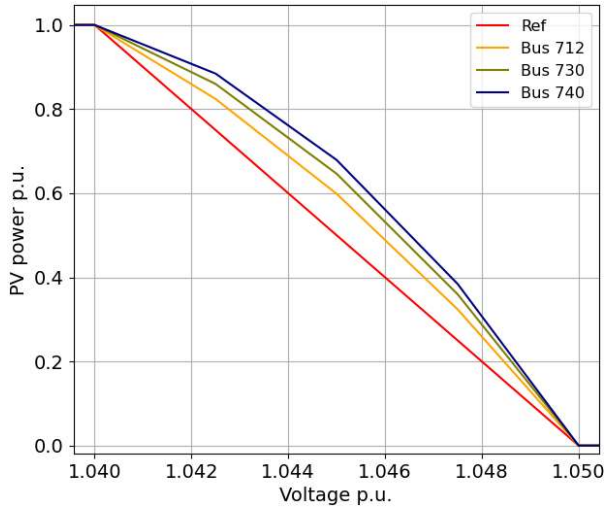

Figure 4.10: Unique DVWC_1 curve for respective PV buses.

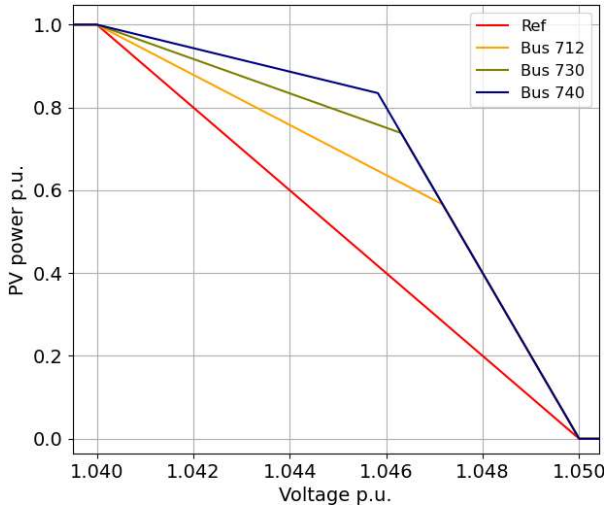

Figure 4.11: Unique DVWC_2 curve for respective PV buses.

4.2.1 One Day PV Data with 1 Hour Resolution

We considered the same PV data for all the PVs for this case study. The PV data is obtained from [52] in a CSV file. The Open-DSS PV model can load PV data from a CSV file and follow the load shape to generate an actual PV profile. Figure 4.12 (a) shows the voltage profile at all the PV nodes when the load is reduced to 35% and Figure 4.12 (b) shows all generated PV power. The PV power production profiles are the same and it is represented

as pu, they look the same. Applying FSC, the voltage reduces as shown in Figure 4.13 (a). Figure 4.13 (b) shows the var support which is identical for all algorithms. Figure 4.14 (a) represents the APC for the FSC method with the highest value being 1 pu meaning 100% generation and the lowest around 80%. So the maximum curtailment is seen to be 20%.

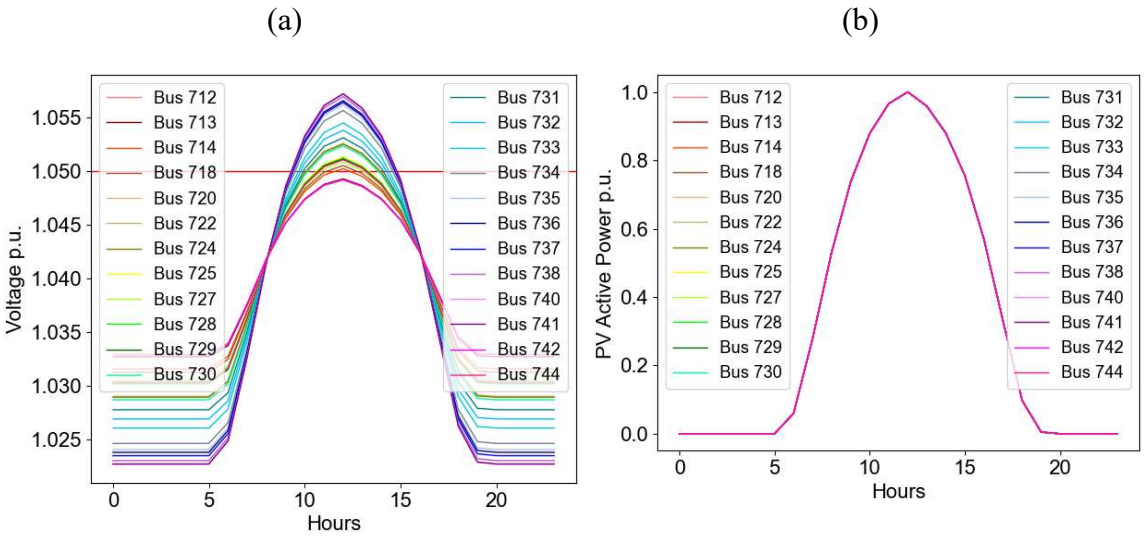

Figure 4.12: (a) Voltage profile and (b) PV profile with no control applied for 35% load.

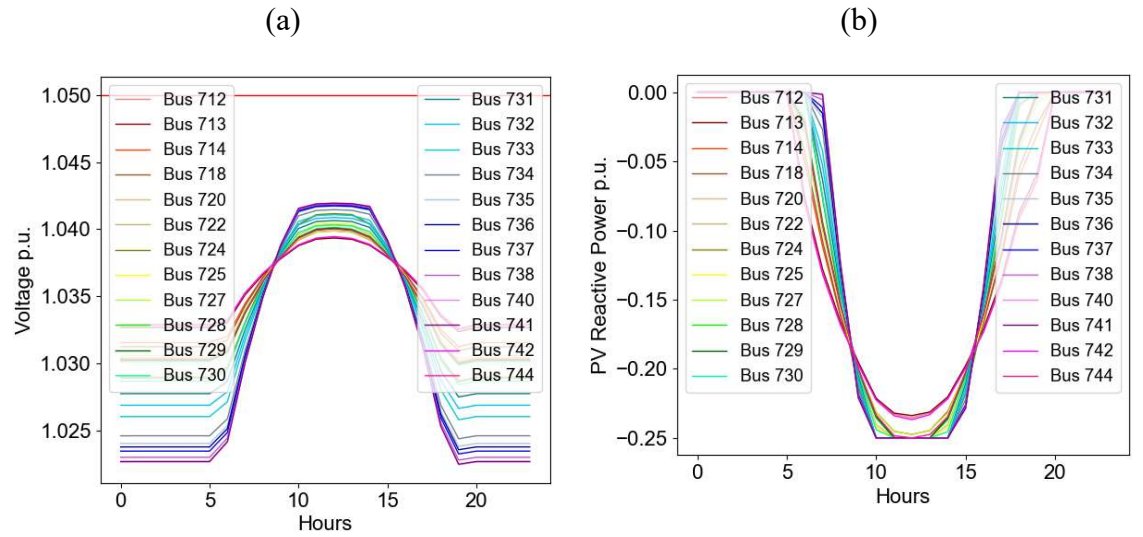

Figure 4.13: (a) Voltage profile and (b) PV profile with FSC applied for 35% load.

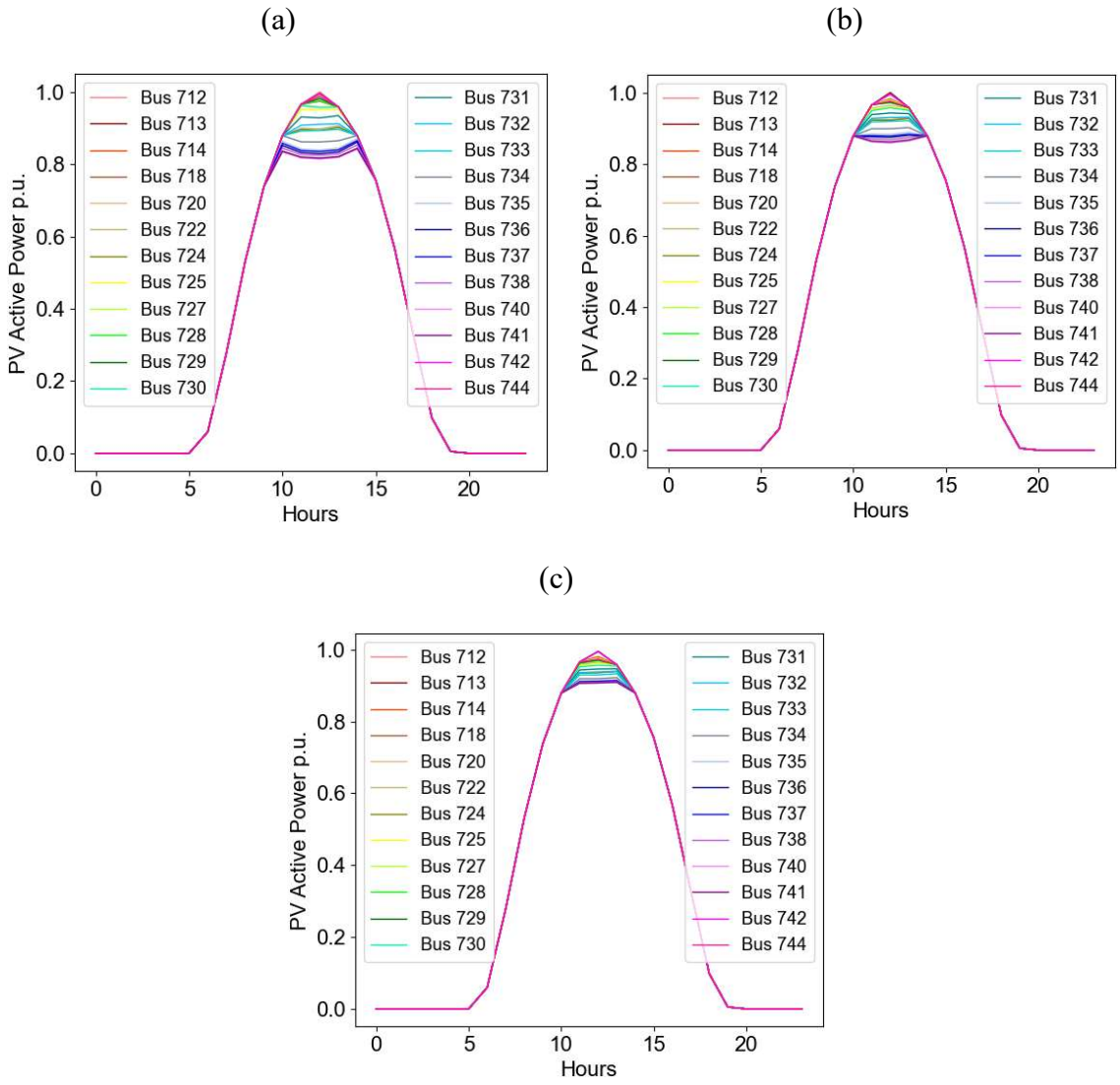

Figure 4.14: APC with (a) FSC, (b) DVWC_1 and (c) DVWC_2 applied for 35% load.

Observing Figure 4.14 (a), we can see FSC resulted in almost 20% curtailment for some PVs, which improved to 15% and 10% in the case of DVWC_1 and DVWC_2 as shown in Figure 4.14 (b) and 4.14 (c). The comparison of variance in Figure 4.15 (a), (b), and (c) shows improvement in fairness for DVWC_1 with half the variance and for DVWC_2 one-fourth than the FSC method.

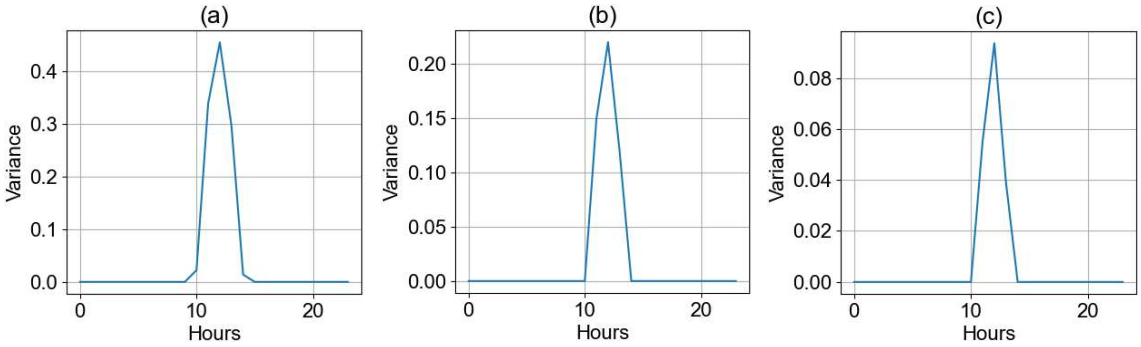

Figure 4.15: Variance with (a) FSC, (b) DVWC_1 and (c) DVWC_2 applied for 35% load.

We then performed a simulation for 25% load. The reactive power absorption gets saturated in this case and results in increased APC. The variance plots in Figure 4.16 show that DVWC_1 and DVWC_2 achieved lower variances and hence better fairness compared to FSC.

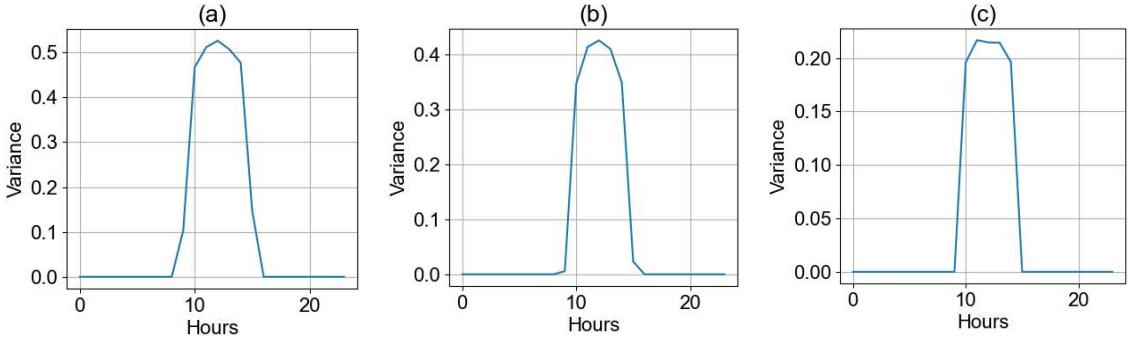

Figure 4.16: Variance with (a) FSC, (b) DVWC_1 and (c) DVWC_2 applied for 25% load.

Figure 4.17 shows the voltage profile with DVWC_2 control when the load is reduced to 15%. We can see the control voltages are over 1.045 pu. The variance results for this case are shown in Figure 4.18. In this case, the DVWC_1 algorithm resulted in higher variance and failed to provide better fairness, rather worse with DVWC_2 control.

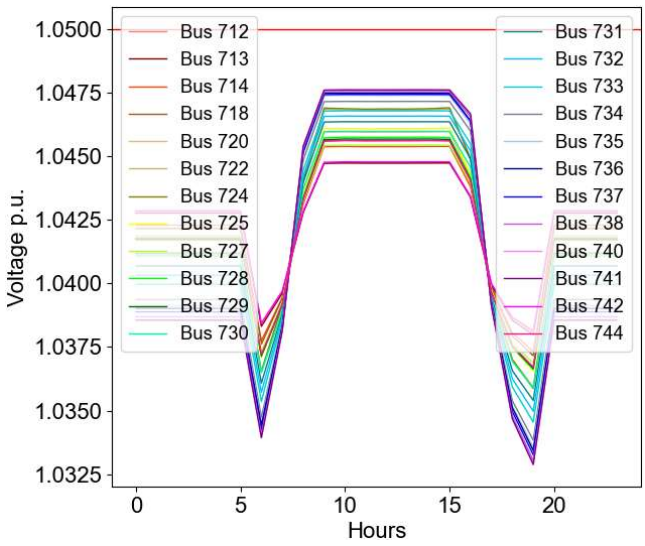

Figure 4.17: Controlled voltage profile with DVWC_2 for 15% load.

This shows the limitations of the DVWC_1 and DVWC_2 algorithms. As voltage rise pushes the controlled voltage beyond 1.045 pu the variance deteriorates. Due to the reduced rate of APC at the beginning of control curves, we had to consider faster APC at the end so that the curves meet at 1.05 pu. This resulted in a steeper slope for higher VSC PVs near 1.05 pu and hence resulted in more APC then expected. Our future work involves improving this limitation.

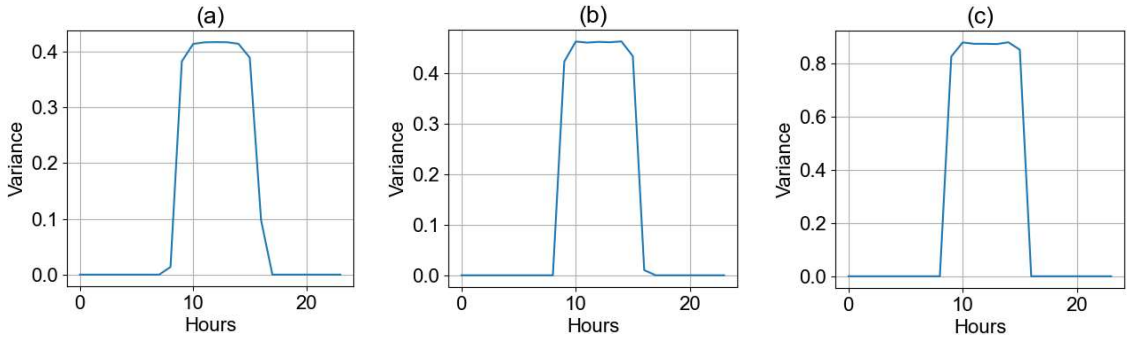

Figure 4.18: Variance with (a) FSC, (b) DVWC_1 and (c) DVWC_2 applied for 15% load.

4.2.2 One Day PV Data with 1 Minute Resolution

We considered different PV data for each PV for this case study to produce the most diverse scenario. The original PV data is obtained from the Open-DSS repository and then used to produce 24 randomized sets of PV data. The data is for one day with a one-minute resolution. Figure 4.19 (a) shows the voltage profile at all the PV nodes when the load is reduced to 30%. Figure 4.19 (b) shows the active power generation of different PVs. When the FSC is applied the voltage reduces as shown in Figure 4.20 (a). Figure 4.20 (b) shows the PV active power with the FSC method, and we can see some curtailment there. Figure 4.20 (c) shows the amount of var support which is the same for all algorithms. The variance values in Figure 4.21 show DVWC_1 method halved the variance than FSC, while DVWC_2 improved fairness with variance four times less than FSC.

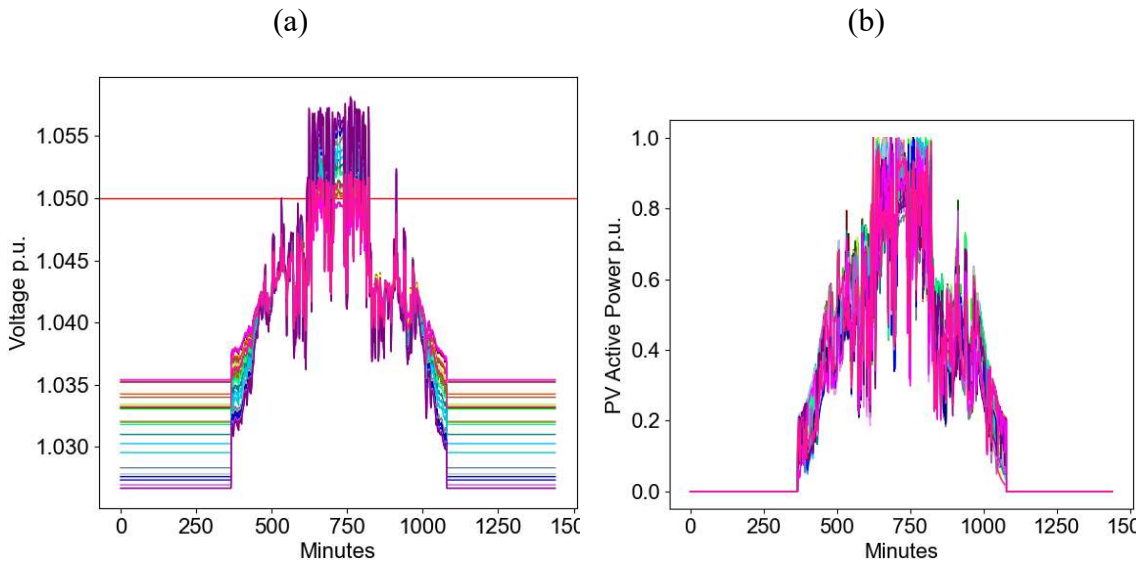

Figure 4.19: Voltage profile with no control for 30% load.

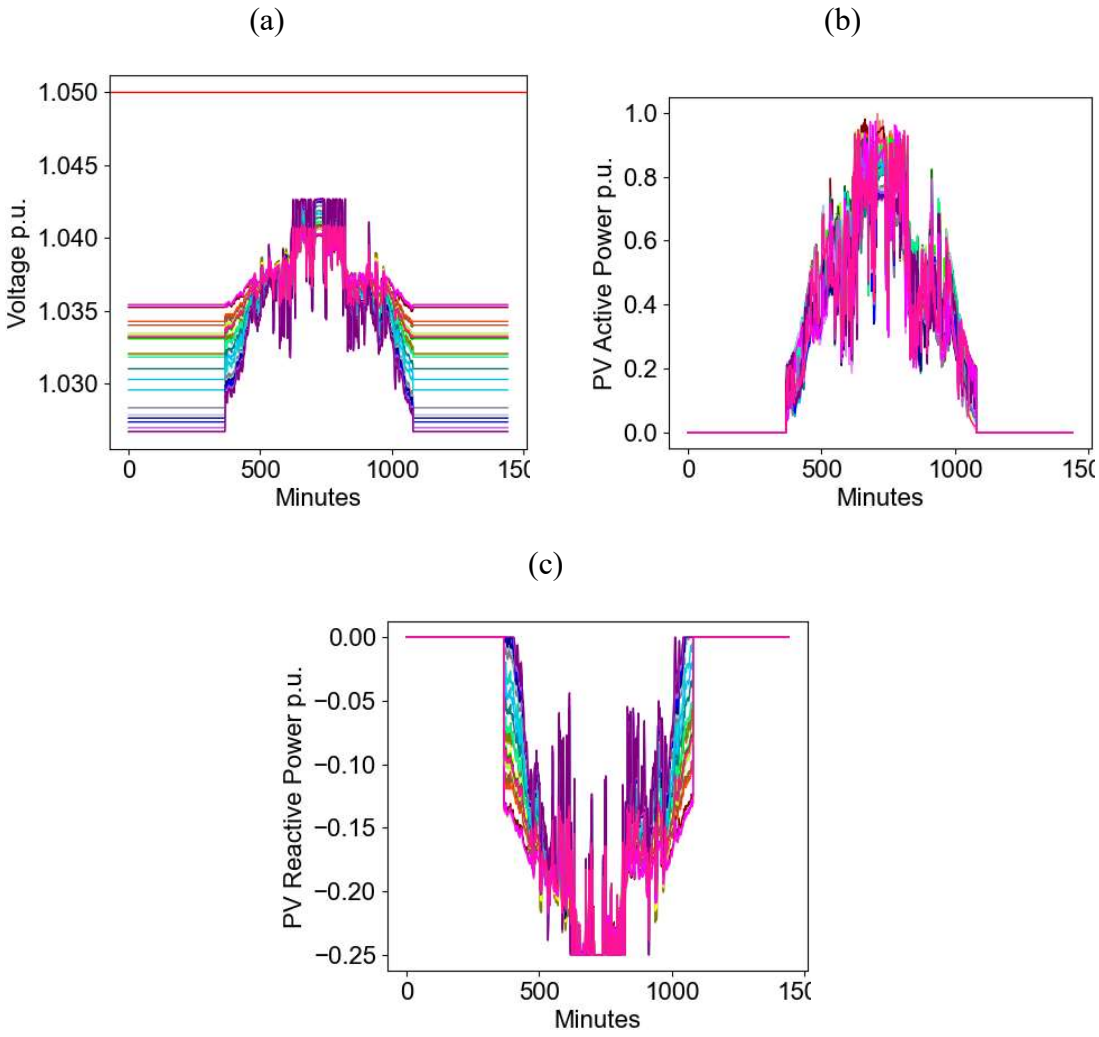

Figure 4.20: (a) Voltage profile, (b) PV profile and (c) var profile with FSC applied for 30% load.

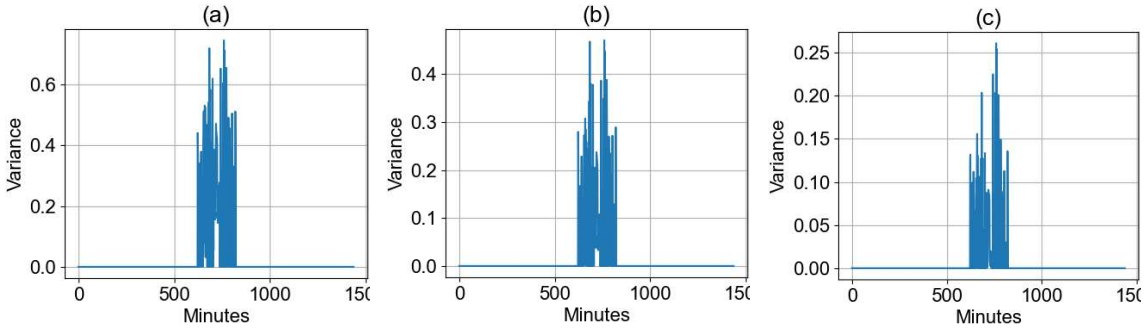

Figure 4.21: Variance with (a) FSC, (b) DVWC_1 and (c) DVWC_2 applied for 30% load.

Figure 4.22 represents variance for the same case study ran above with load reduced to 25%. Like the previous results analyzed in section 4.2.1, the effectiveness of fairness algorithms is reduced with the reduction in load. DVWC_1 achieved little improvement in this case, while DVWC_2 still improved fairness with half the variance than FSC.

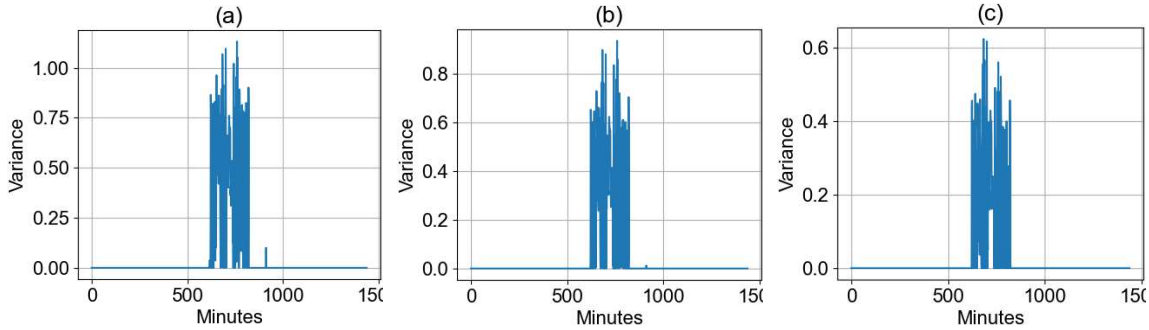

Figure 4.22: Variance for (a) FSC, (b) DVWC_1 and (c) DVWC_2 for 25% load.

4.2.3 Effect of Informed Addition/Removal of PV on VSCs and DVWC Algorithms

We considered this scenario to show how DVWC curves can be updated when some PV is removed/added to the system with prior notice from the customer. With the same PV profiles as 4.2.2, we consider a situation when the PV at bus 722 gets disconnected at minute 600 and reconnects at minute 720. Another PV on bus 735 gets connected at minute 721 and disconnected at minute 840. We considered this to be informed changes. Therefore, for each instance, we recalculate VSCs and reconfigure the SI parameters for DVWCs accordingly. With load at 25%, the voltage profile with no control is shown in Figure 4.23 (a), with voltage rising most during minutes 721-840 when all PVs are generating power. Corresponding PV profiles are shown in Figure 4.23 (b), and the profile for PV at bus 722 is presented in Figure 4.23 (c) to show it is off from 601-720 minutes.

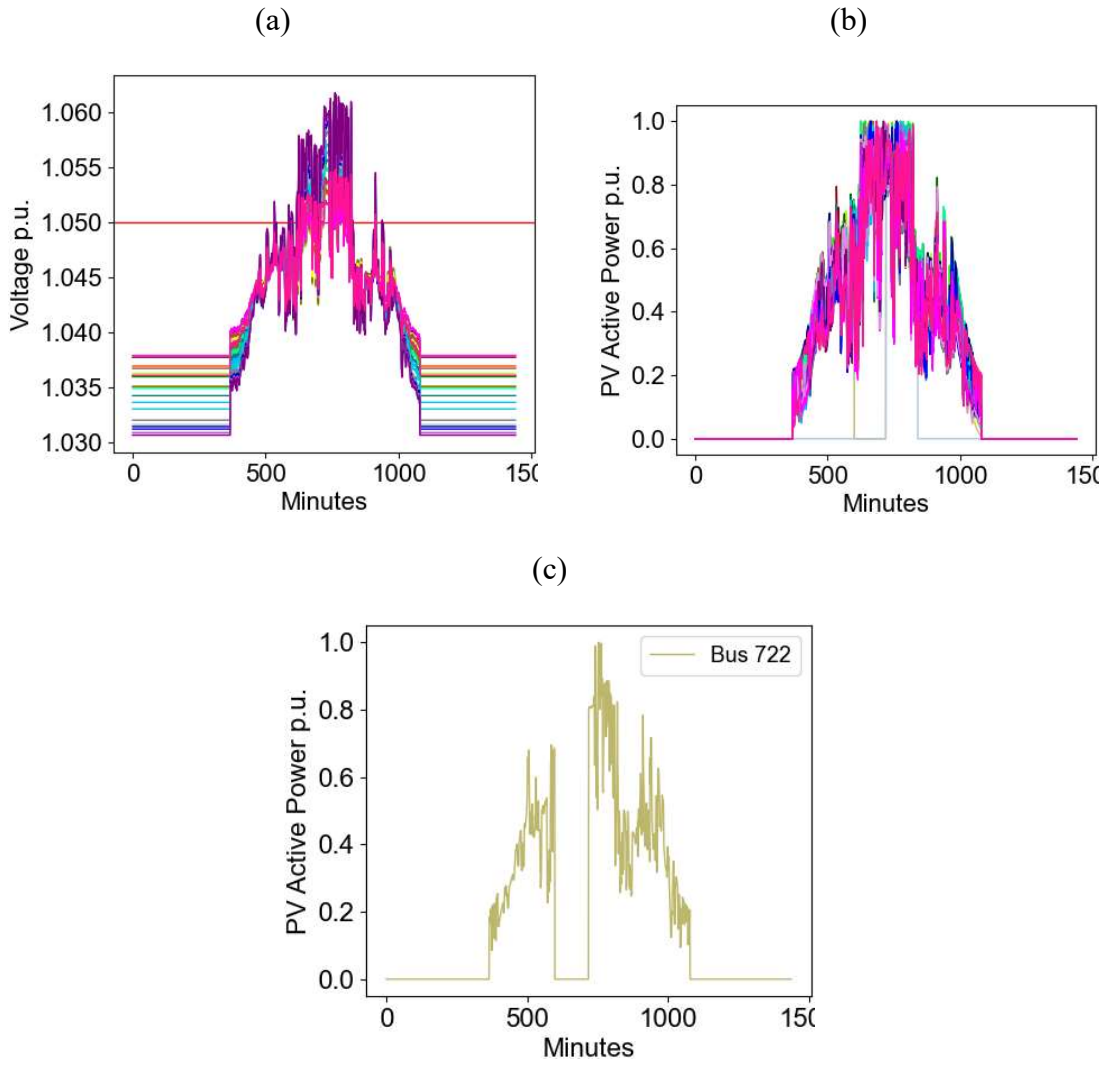

Figure 4.23: Voltage profile with no control for 25% load.

As it is informed change of the number of PV units, the system calculates the VSCs before the occurrence of the event and updates DVWC curves. VSC calculation only takes consideration of the PVs that are connected and updates the droop curves. So, there is no coefficient calculation for PV at bus 735 except for minutes 721-840. The recalculated VSCs are shown in Table 4.2.

Table 4.2: Calculated VSCs for changes in system configuration.

Bus	kVA	kW	R_{cof} (0-600)	R_{cof} (601-720)	R_{cof} (721-840)	R_{cof} (841-1440)
712	76.5	68.85	0.01593	0.01467	0.01651	0.01593
713	76.5	68.85	0.0163	0.01454	0.01689	0.0163
714	34.2	30.78	0.01838	0.01599	0.01901	0.01838
718	76.5	68.85	0.01901	0.0166	0.01962	0.01901
720	76.5	68.85	0.02045	0.01702	0.02108	0.02045
722	144.9	130.41	0.02324		0.02388	0.02324
724	37.8	34.02	0.02343	0.01801	0.02403	0.02343
725	37.8	34.02	0.02084	0.01738	0.02144	0.02084
727	37.8	34.02	0.01968	0.01839	0.02062	0.01968
728	113.4	102.06	0.02049	0.01926	0.02144	0.02049
729	37.8	34.02	0.02034	0.01905	0.02125	0.02034
730	76.5	68.85	0.02275	0.02149	0.0241	0.02275
731	76.5	68.85	0.02436	0.02312	0.02578	0.02436
732	37.8	34.02	0.02575	0.0245	0.02743	0.02575
733	76.5	68.85	0.02703	0.02581	0.02897	0.02703
734	37.8	34.02	0.02933	0.02806	0.0316	0.02933
735	76.5	68.85			0.03272	
736	37.8	34.02	0.03033	0.02912	0.03323	0.03033
737	126	113.4	0.03141	0.03021	0.0337	0.03141
738	113.4	102.06	0.03226	0.03104	0.03456	0.03226
740	76.5	68.85	0.03293	0.03173	0.03523	0.03293
741	37.8	34.02	0.03284	0.03164	0.03511	0.03284
742	83.7	75.33	0.01599	0.0148	0.01665	0.01599
744	37.8	34.02	0.02016	0.01892	0.02108	0.02016

The variance values presented in Figure 4.24 show DVWC_1 achieved a 20% reduction in variance and DVWC_2 achieved a 50% reduction overall compared to FSC method. Therefore, the algorithms were successful in maintaining improved fairness under the same load conditions with PVs going on and off.

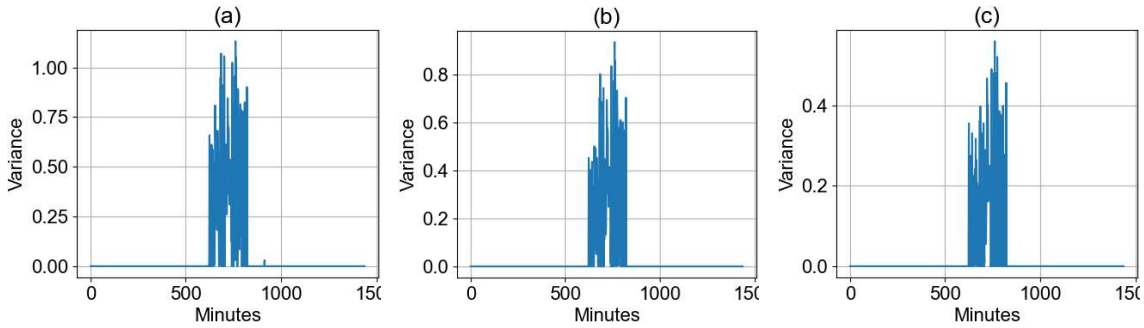

Figure 4.24: Variance with (a) FSC, (b) DVWC_1 and (c) DVWC_2 applied for 25% load when VSC is updated with PV unit going on/off.

4.2.4 Effect of Uninformed Addition/Removal of PV on VSCs and DVWC Algorithms

We considered the same situation as section 4.2.3 with the exception that the add/remove condition is uninformed. This results in VSCs not to be recalculated and DVWC curves remain the same. The resulting variance is shown in Figure 4.25. Note that there is very little to no change in fairness achievement compared to the results in section 4.2.3. Thus, even if VSC updates are delayed due to communication failures, or a few PVs go on and off without notice, the system can still maintain a similar level of fairness.

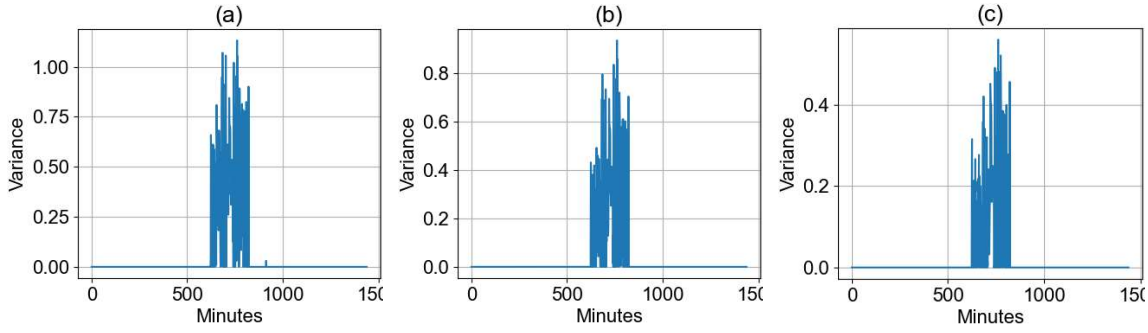

Figure 4.25: Variance with (a) FSC, (b) DVWC_1 and (c) DVWC_2 applied for 25% load when VSC is not updated.

4.3 Limitations

Despite providing a better result in fairness improvement, there are several limitations in our proposed methods. These are listed below:

1. We couldn't generate any unique control curve for coefficients less than .0043 for DVWC_1 and less than .01 for DVWC_2. For DVWC_1 VSC less than .0043 results in a control curve with APC > 50% for the .0025 voltage range which may result in oscillation of the voltage. In the case of DVWC_2, there is no intersection for VSC less than .01. This resulted in a fixed curve for PVs that are connected to those buses.

2. Our focus was to slow down the rate of APC for PVs with larger VSC, allowing the later PV nodes to enter the control region. Therefore, in the case of both DVWC algorithms, we have a slower slope at the beginning of the control curve. As a result, at the end of the curve i.e. near 1.05 pu, the slope of the curve is steeper, causing a higher rate of APC for PVs with higher VSC. That is why as the control voltage reaches nearly 1.05 pu the performance of the DVWC algorithms deteriorates.

3. The DVWC algorithms are only effective when PV integration is more than 50% of the maximum load rating. When PV integration is less than 50%, voltage rise at some buses doesn't follow the sequence of the VSC values as noticed in Table 3.4. As a result, the performance of the DVWC algorithms was not as good as expected.

Chapter 5

Conclusion

This chapter summarizes the work done in the previous chapters based on the results obtained and highlights opportunities for future research.

5.1 Summary

In this thesis, we have investigated typical radial power system models with communication capability. The focus of this thesis is to investigate the capabilities of SIs in regulating voltage at low-voltage distribution feeders through active/reactive power support. Our analysis showed that the conventional volt-var-watt method causes unnecessary APC, reduces total PV generation, and is not capable of achieving fair APC. In contrast, our proposed methods reduce total APC and improve fairness. The variance results show an improvement in fairness for both DVWC algorithms in most cases. Test scenarios performed in IEEE 37-bus also validate the effectiveness of the proposed algorithms.

We have also presented a perturb and observe method to calculate VSCs that can provide insight into the voltage rise of each bus node due to changes in all PV's generation. The VSCs represent the influence of neighboring PVs and can be an indicator of which bus voltages are going to cross the lower control voltage range first under low load conditions.

Also, it can easily work with distributed communication infrastructure. Compared to a centralized system, our method requires less communication frequency and updates.

We presented simulation results for PVs having identical generation profiles and also with a diversity of profiles. In both cases, our algorithms achieved better fairness than the FSC method. Though it is very unlikely for PVs to have such a difference in generation within a small area, we considered the highest possibility of difference in generation to show the effectiveness of our proposed algorithms. The SI parameters in our proposed algorithm only need to be updated as per changes in system configuration. Yet we showed results where failure to update SI parameters doesn't affect the performance of the algorithms much. This may not be the case if large numbers of PV units connect to/disconnect simultaneously from the system.

Despite achieving improved fairness, we encountered certain limitations to our algorithms. The most important drawback is the lack of fairness around the upper control voltage range, v_{ch}. We believe having different v_{ch} will reduce the difference in slope steepness. However, calculating how much difference is appropriate requires further research. Nevertheless, the DVWC algorithms performed better for most of the control regions. Though we evaluated the applicability of the algorithms in simulation only, the research in the future may be expanded with experimental results to pave the way towards real-world applicability.

5.2 Future Work

There is significant potential for extension of the research ideas presented in this thesis. That includes:

1. Improvement of fairness when node voltage deviation approaches or exceeds the upper limit.

2. Developing a dynamic volt-var control strategy that incorporates fairness in reactive power absorption.

3. Implementation of the algorithms in unbalanced systems, both three-phase and single phase. This may involve using actual system data of loads, lines, generators, and PVs so that we can evaluate whether the algorithms can be applied in a real-world scenario.

4. Design and implement fairness algorithms in a lab environment and evaluate experimental results with simulation results. This will allow further editions required to apply these algorithms in real-world scenarios.

Appendix: A

A typical system with three loads and three PV units is presented in Figure A.1. Here equal loads of 5 MW and 1.64 MVar are connected to buses A, B, and C, each with an 8 MVA PV unit. With load reduced to 70%, we can notice overvoltage at buses C and D as shown in Figure A.2 (a) considering the overvoltage constraint is 1.05 pu. All three PVs generate maximum power without any external control as shown in Figure A.2 (b). All the system specifications including PV data are obtained from [52].

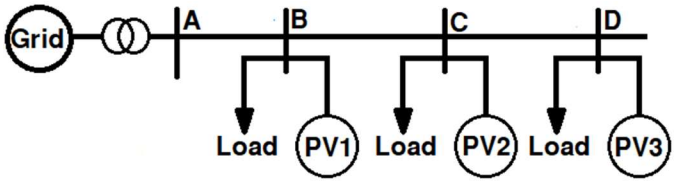

Figure A.1: Typical distribution system.

(a) (b)

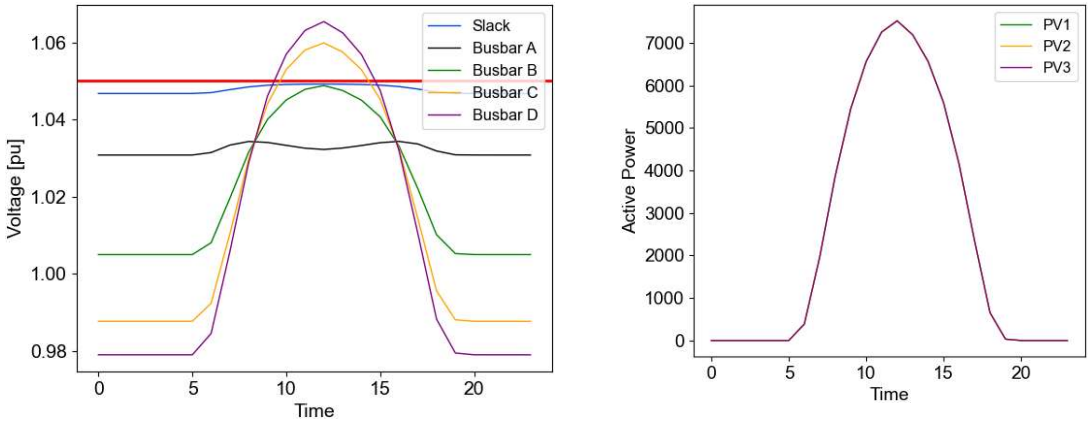

Figure A.2: Bus voltages no control.

We can apply volt-watt control in this system to regulate voltage. Figure A.3 (a) shows the volt-watt curve parameters, where $V_1 = 1.04$ pu is when PV will start curtailment to reduce voltage And $V_2 = 1.05$ pu is the permissible voltage upper limit. In Figure A.3 (b) we can see the voltage is successfully controlled, but it causes APC as shown in Figure A.4 (a).

(a) (b)

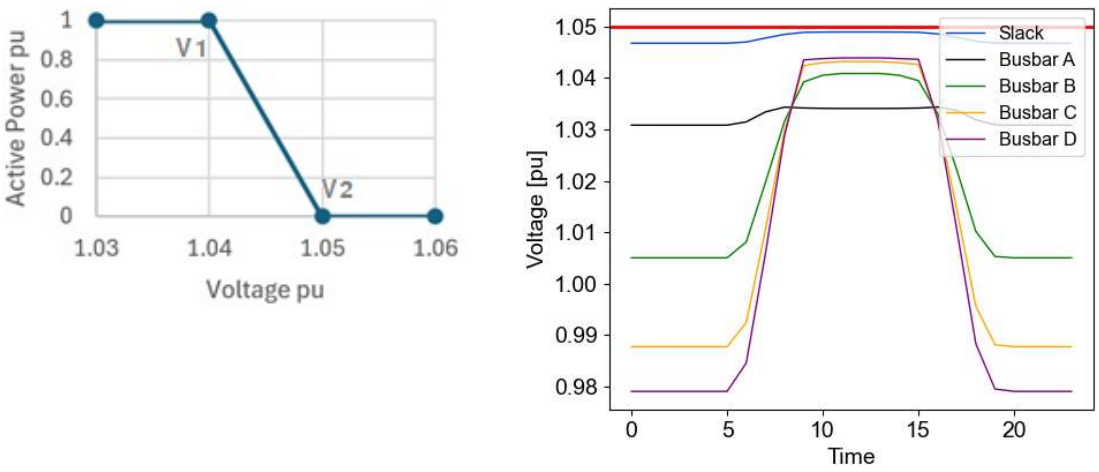

Figure A.3: (a)Volt-watt curve for FSC and (b) resulting bus voltages.

We can see the curtailment is unfair allowing PV1 to generate almost 2.5 MW more power than PV3. If we change V1 to 1.045 the amount of curtailment changes allowing more PV power generation for each PV as shown in Figure A.4 (b), but the unfairness persists. This observation shows that choosing different parameters for PVs can allow different generation capabilities of the PVs, which can lead to improved fairness.

(a) (b)

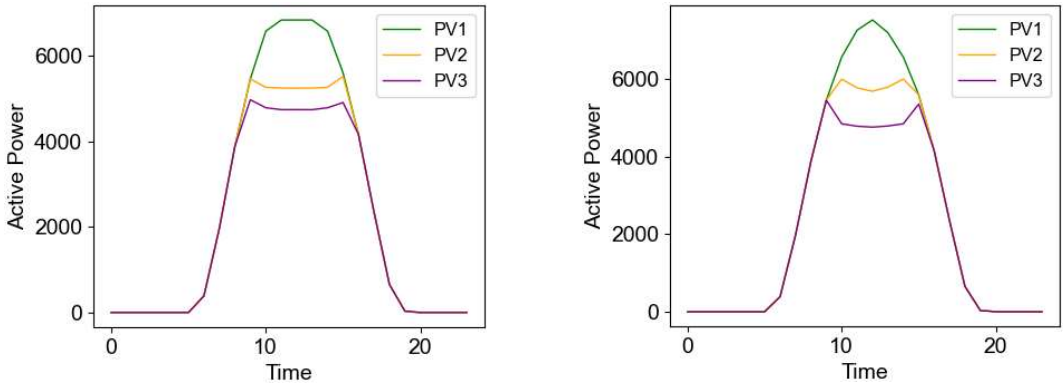

Figure A.4: PV output for SI parameter of volt-watt curve (a) 1.04-1.05 pu and (b) 1.045-1.05 pu.

References

[1] "Renewable Energy Progress Tracker – Data Tools," IEA. Accessed: Sep. 13, 2024. [Online]. Available: https://www.iea.org/data-and-statistics/data-tools/renewable-energy-progress-tracker

[2] D. T. Rizy, H. Li, F. Li, Y. Xu, S. Adhikari, and P. Irminger, "Impacts of varying penetration of distributed resources with & without volt/var control: Case study of varying load types," in *2011 IEEE Power and Energy Society General Meeting*, Jul. 2011, pp. 1–7. doi: 10.1109/PES.2011.6039014.

[3] A. Dubey, S. Santoso, and M. P. Cloud, "Understanding the effects of electric vehicle charging on the distribution voltages," in *2013 IEEE Power & Energy Society General Meeting*, Vancouver, BC: IEEE, 2013, pp. 1–5. doi: 10.1109/PESMG.2013.6672557.

[4] J. O. Petinrin and M. Shaabanb, "Impact of renewable generation on voltage control in distribution systems," *Renew. Sustain. Energy Rev.*, vol. 65, pp. 770–783, Nov. 2016, doi: 10.1016/j.rser.2016.06.073.

[5] Y.-J. Liu, Y.-H. Tai, C.-Y. Huang, H.-J. Su, P.-H. Lan, and M.-K. Hsieh, "Assessment of the PV hosting capacity for the medium-voltage 11.4 kV distribution feeder," in *2018 IEEE International Conference on Applied System Invention (ICASI)*, Chiba: IEEE, Apr. 2018, pp. 381–384. doi: 10.1109/ICASI.2018.8394262.

[6] I. Andrade, R. Pena, R. Blasco-Gimenez, J. Riedemann, W. Jara, and C. Pesce G., "An Active/Reactive Power Control Strategy for Renewable Generation Systems," *Electronics*, vol. 10, p. 1061, Apr. 2021, doi: 10.3390/electronics10091061.

[7] B. Enayati, "Impact of IEEE 1547 Standard on Smart Inverters and the Applications in Power Systems," 2020.

[8] "IEEE Standard for Interconnection and Interoperability of Distributed Energy Resources with Associated Electric Power Systems Interfaces," *IEEE Std 1547-2018 Revis. IEEE Std 1547-2003*, pp. 1–138, Apr. 2018, doi: 10.1109/IEEESTD.2018.8332112.

[9] M. Z. Liu *et al.*, "On the Fairness of PV Curtailment Schemes in Residential Distribution Networks," *IEEE Trans. Smart Grid*, vol. 11, no. 5, pp. 4502–4512, Sep. 2020, doi: 10.1109/TSG.2020.2983771.

[10] A. T. Procopiou, K. Petrou, L. F. Ochoa, T. Langstaff, and J. Theunissen, "Adaptive Decentralized Control of Residential Storage in PV-Rich MV–LV Networks," *IEEE Trans. Power Syst.*, vol. 34, no. 3, pp. 2378–2389, May 2019, doi: 10.1109/TPWRS.2018.2889843.

[11] M. Rankin, "Export limits for Embedded Generators up to 200kVA connected at Low Voltage," *AusNet Serv.*, Jul. 2017.

[12] M. M. Haque and P. Wolfs, “A review of high PV penetrations in LV distribution networks: Present status, impacts and mitigation measures,” *Renew. Sustain. Energy Rev.*, vol. 62, pp. 1195–1208, Sep. 2016, doi: 10.1016/j.rser.2016.04.025.

[13] Y. P. Agalgaonkar, B. C. Pal, and R. A. Jabr, “Distribution Voltage Control Considering the Impact of PV Generation on Tap Changers and Autonomous Regulators,” *IEEE Trans. Power Syst.*, vol. 29, no. 1, pp. 182–192, Jan. 2014, doi: 10.1109/TPWRS.2013.2279721.

[14] J. Watson, N. Watson, and B. Das, “Effectiveness of Power Electronic Voltage Regulators in the Distribution Network,” *IET Gener. Transm. Distrib.*, vol. 10, Aug. 2016, doi: 10.1049/iet-gtd.2016.0300.

[15] A. Singhal, V. Ajjarapu, J. Fuller, and J. Hansen, “Real-Time Local Volt/Var Control Under External Disturbances With High PV Penetration,” *IEEE Trans. Smart Grid*, vol. 10, no. 4, pp. 3849–3859, Jul. 2019, doi: 10.1109/TSG.2018.2840965.

[16] S. Jothibasu, S. Santoso, and A. Dubey, “Determining PV hosting capacity without incurring grid integration cost,” in *2016 North American Power Symposium (NAPS)*, Sep. 2016, pp. 1–5. doi: 10.1109/NAPS.2016.7747939.

[17] M. Deakin and M. McCulloch, “Voltage regulation of large scale PV: A comparative case study,” in *2017 IEEE Manchester PowerTech*, Jun. 2017, pp. 1–6. doi: 10.1109/PTC.2017.7981021.

[18] Y. Wang, K. T. Tan, X. Y. Peng, and P. L. So, “Coordinated Control of Distributed Energy-Storage Systems for Voltage Regulation in Distribution Networks,” *IEEE Trans. Power Deliv.*, vol. 31, no. 3, pp. 1132–1141, Jun. 2016, doi: 10.1109/TPWRD.2015.2462723.

[19] B. Mirafzal and A. Adib, “On Grid-Interactive Smart Inverters: Features and Advancements,” *IEEE Access*, vol. 8, pp. 160526–160536, 2020, doi: 10.1109/ACCESS.2020.3020965.

[20] B. Arbab-Zavar, E. J. Palacios-Garcia, J. C. Vasquez, and J. M. Guerrero, “Smart Inverters for Microgrid Applications: A Review,” *Energies*, vol. 12, no. 5, Art. no. 5, Jan. 2019, doi: 10.3390/en12050840.

[21] H. Nazaripouya, H. R. Pota, C.-C. Chu, and R. Gadh, “Real-Time Model-Free Coordination of Active and Reactive Powers of Distributed Energy Resources to Improve Voltage Regulation in Distribution Systems,” *IEEE Trans. Sustain. Energy*, vol. 11, no. 3, pp. 1483–1494, Jul. 2020, doi: 10.1109/TSTE.2019.2928824.

[22] M. Rashid and A. M. Knight, “Combining Volt/Var & Volt/Watt modes to increase PV hosting capacity in LV distribution networks,” in *2020 IEEE Electric Power and Energy Conference (EPEC)*, Nov. 2020, pp. 1–5. doi: 10.1109/EPEC48502.2020.9319927.

[23] J. Seuss, M. J. Reno, R. J. Broderick, and S. Grijalva, "Improving distribution network PV hosting capacity via smart inverter reactive power support," in *2015 IEEE Power & Energy Society General Meeting*, Jul. 2015, pp. 1–5. doi: 10.1109/PESGM.2015.7286523.

[24] A. M. S. Alonso, L. D. O. Arenas, D. I. Brandao, E. Tedeschi, and F. P. Marafao, "Integrated Local and Coordinated Overvoltage Control to Increase Energy Feed-In and Expand DER Participation in Low-Voltage Networks," *IEEE Trans. Sustain. Energy*, vol. 13, no. 2, pp. 1049–1061, Apr. 2022, doi: 10.1109/TSTE.2022.3146196.

[25] W. Ma, W. Wang, Z. Chen, and R. Hu, "A centralized voltage regulation method for distribution networks containing high penetrations of photovoltaic power," *Int. J. Electr. Power Energy Syst.*, vol. 129, p. 106852, Jul. 2021, doi: 10.1016/j.ijepes.2021.106852.

[26] A. Inaolaji, A. Savasci, and S. Paudyal, "Distribution Grid Optimal Power Flow with Volt-VAr and Volt-Watt Settings of Smart Inverters," in *2021 IEEE Industry Applications Society Annual Meeting (IAS)*, Vancouver, BC, Canada: IEEE, Oct. 2021, pp. 1–7. doi: 10.1109/IAS48185.2021.9715792.

[27] H. Lee, J.-C. Kim, and S.-M. Cho, "Optimal Volt–Var Curve Setting of a Smart Inverter for Improving Its Performance in a Distribution System," *IEEE Access*, vol. 8, pp. 157931–157945, 2020, doi: 10.1109/ACCESS.2020.3019794.

[28] T. O. Olowu, A. Inaolaji, A. Sarwat, and S. Paudyal, "Optimal Volt-VAR and Volt-Watt Droop Settings of Smart Inverters," in *2021 IEEE Green Technologies Conference (GreenTech)*, Apr. 2021, pp. 89–96. doi: 10.1109/GreenTech48523.2021.00025.

[29] M. M. Viyathukattuva Mohamed Ali, P. H. Nguyen, W. L. Kling, A. I. Chrysochos, T. A. Papadopoulos, and G. K. Papagiannis, "Fair power curtailment of distributed renewable energy sources to mitigate overvoltages in low-voltage networks," in *2015 IEEE Eindhoven PowerTech*, Jun. 2015, pp. 1–5. doi: 10.1109/PTC.2015.7232796.

[30] Q. Zhou, M. Shahidehpour, A. Paaso, S. Bahramirad, A. Alabdulwahab, and A. Abusorrah, "Distributed Control and Communication Strategies in Networked Microgrids," *IEEE Commun. Surv. Tutor.*, vol. 22, no. 4, pp. 2586–2633, 2020, doi: 10.1109/COMST.2020.3023963.

[31] F. Nawaz, E. Pashajavid, Y. Fan, and M. Batool, "A Comprehensive Review of the State-of-the-Art of Secondary Control Strategies for Microgrids," *IEEE Access*, vol. 11, pp. 102444–102459, 2023, doi: 10.1109/ACCESS.2023.3316016.

[32] C. Zhang, X. Dou, L. Wang, Y. Dong, and Y. Ji, "Distributed Cooperative Voltage Control for Grid-Following and Grid-Forming Distributed Generators in Islanded Microgrids," *IEEE Trans. Power Syst.*, vol. 38, no. 1, pp. 589–602, Jan. 2023, doi: 10.1109/TPWRS.2022.3158306.

[33] A. Joseph, K. Smedley, and S. Mehraeen, “Secure High DER Penetration Power Distribution via Autonomously Coordinated Volt/VAR Control,” *IEEE Trans. Power Deliv.*, vol. 35, no. 5, pp. 2272–2284, Oct. 2020, doi: 10.1109/TPWRD.2020.2965107.

[34] L. Collins and J. K. Ward, “Real and reactive power control of distributed PV inverters for overvoltage prevention and increased renewable generation hosting capacity,” *Renew. Energy*, vol. 81, pp. 464–471, Sep. 2015, doi: 10.1016/j.renene.2015.03.012.

[35] J. Noh, S. Kang, J. Kim, and J.-W. Park, “A Study on Volt-Watt Mode of Smart Inverter to Prevent Voltage Rise with High Penetration of PV System,” in *2019 IEEE Power & Energy Society General Meeting (PESGM)*, Aug. 2019, pp. 1–5. doi: 10.1109/PESGM40551.2019.8973860.

[36] S. Yoshizawa *et al.*, “Voltage-Sensitivity-Based Volt-VAR-Watt Settings of Smart Inverters for Mitigating Voltage Rise in Distribution Systems,” *IEEE Open Access J. Power Energy*, vol. 8, pp. 584–595, 2021, doi: 10.1109/OAJPE.2021.3125013.

[37] R. K. Gupta and D. K. Molzahn, “Analysis of Fairness-promoting Optimization Schemes of Photovoltaic Curtailments for Voltage Regulation in Power Distribution Networks,” Mar. 30, 2024, *arXiv*: arXiv:2404.00394. doi: 10.48550/arXiv.2404.00394.

[38] M. G. Kashani, M. Mobarrez, and S. Bhattacharya, “Smart Inverter Volt-Watt Control Design in High PV-Penetrated Distribution Systems,” *IEEE Trans. Ind. Appl.*, vol. 55, no. 2, pp. 1147–1156, Mar. 2019, doi: 10.1109/TIA.2018.2878844.

[39] A. N. M. M. Haque, M. Xiong, and P. H. Nguyen, “Consensus Algorithm for Fair Power Curtailment of PV Systems in LV Networks,” in *2019 IEEE PES GTD Grand International Conference and Exposition Asia (GTD Asia)*, Mar. 2019, pp. 813–818. doi: 10.1109/GTDAsia.2019.8715912.

[40] J. Seuss, M. J. Reno, M. Lave, R. J. Broderick, and S. Grijalva, “Advanced inverter controls to dispatch distributed PV systems,” in *2016 IEEE 43rd Photovoltaic Specialists Conference (PVSC)*, Jun. 2016, pp. 1387–1392. doi: 10.1109/PVSC.2016.7749842.

[41] J. H. Braslavsky, L. D. Collins, and J. K. Ward, “Voltage Stability in a Grid-Connected Inverter With Automatic Volt-Watt and Volt-VAR Functions,” *IEEE Trans. Smart Grid*, vol. 10, no. 1, pp. 84–94, Jan. 2019, doi: 10.1109/TSG.2017.2732000.

[42] T. T. Mai, N. A. N. M. M. Haque, H. T. Vo, and P. H. Nguyen, “Coordinated active and reactive power control for overvoltage mitigation in physical LV microgrids,” *J. Eng.*, vol. 2019, no. 18, pp. 5007–5011, Jul. 2019, doi: 10.1049/joe.2018.9355.

[43] G. C. Kryonidis, E. O. Kontis, A. I. Chrysochos, C. S. Demoulias, and G. K. Papagiannis, “A Coordinated Droop Control Strategy for Overvoltage Mitigation in Active Distribution Networks,” *IEEE Trans. Smart Grid*, vol. 9, no. 5, pp. 5260–5270, Sep. 2018, doi: 10.1109/TSG.2017.2685686.

[44] G. Cavraro, T. Caldognetto, R. Carli, and P. Tenti, “A Master/Slave Approach to Power Flow and Overvoltage Control in Low-Voltage Microgrids,” *Energies*, vol. 12, no. 14, Art. no. 14, Jan. 2019, doi: 10.3390/en12142760.

[45] S. Poudel, M. Mukherjee, R. Sadnan, and A. P. Reiman, “Fairness-Aware Distributed Energy Coordination for Voltage Regulation in Power Distribution Systems,” *IEEE Trans. Sustain. Energy*, vol. 14, no. 3, pp. 1866–1880, Jul. 2023, doi: 10.1109/TSTE.2023.3252944.

[46] Z. Wei, F. De Nijs, J. Li, and H. Wang, “Model-Free Approach to Fair Solar PV Curtailment Using Reinforcement Learning,” in *Proceedings of the 14th ACM International Conference on Future Energy Systems*, Orlando FL USA: ACM, Jun. 2023, pp. 14–21. doi: 10.1145/3575813.3576871.

[47] A. Inaolaji, A. Savasci, and S. Paudyal, “Distribution Grid Optimal Power Flow in Unbalanced Multiphase Networks With Volt-VAr and Volt-Watt Droop Settings of Smart Inverters,” *IEEE Trans. Ind. Appl.*, vol. 58, no. 5, pp. 5832–5843, Sep. 2022, doi: 10.1109/TIA.2022.3181110.

[48] Y. Z. Gerdroodbari, R. Razzaghi, and F. Shahnia, “Decentralized Control Strategy to Improve Fairness in Active Power Curtailment of PV Inverters in Low-Voltage Distribution Networks,” *IEEE Trans. Sustain. Energy*, vol. 12, no. 4, pp. 2282–2292, Oct. 2021, doi: 10.1109/TSTE.2021.3088873.

[49] Paulo Radatz, Celso Rocha, Wes Sunderman, Matthew Rylander, and Jouni Peppanen, “OpenDSS PVSystem and InvControl Element Models.” Electrical Power Research Institute (EPRI), Aug. 2020.

[50] J. Smith, “Modeling High-Penetration PV for Distribution Interconnection Studies: Smart Inverter Function Modeling in OpenDSS, Rev 3,” *Electr. Power Res. Inst. EPRI*, May 2017.

[51] C.-H. Lo and N. Ansari, “Decentralized Controls and Communications for Autonomous Distribution Networks in Smart Grid,” *IEEE Trans. Smart Grid*, vol. 4, no. 1, pp. 66–77, Mar. 2013, doi: 10.1109/TSG.2012.2228282.

[52] “Prof Luis (Nando) Ochoa - Research Tools.” Accessed: Sep. 14, 2024. [Online]. Available: https://sites.google.com/view/luisfochoa/research-tools

Curriculum Vitae

Name: Shafait Ahmed

Education: Bachelor of Science in Electrical and Electronic Engineering

International Islamic University Chittagong, Chattogram, Bangladesh.

February 2007 – June 2011

Publications:

1. S. Ahmed, T. Rahimi, J. L. Cardenas-Barrera, Z. A. Khan and C. Diduch, "Quadratic-Equation Based Volt-Watt Control Rules Design Strategy to Mitigate Overvoltage in Power Grids with High Penetration of Solar Sources," *2024 IEEE 12th International Conference on Smart Energy Grid Engineering (SEGE)*, Oshawa, ON, Canada, 2024, pp. 200-205, doi: 10.1109/SEGE62220.2024.10739555.

2. Z. A. Khan, T. Rahimi, J. L. Cardenas-Barrera, S. Ahmed and C. Diduch, "Optimal Smart Inverter Volt-Watt and Volt-Var Settings to Maximize Fair Contribution in Voltage Regulation," *2024 IEEE 12th International Conference on Smart Energy Grid Engineering (SEGE)*, Oshawa, ON, Canada, 2024, pp. 31-36, doi: 10.1109/SEGE62220.2024.10739597.

3. K. A. A. Mamun, N. Islam, E. H. Raju, S. A. Abir, M. A. U. Zaman and S. Ahmed, "Design and Simulation of SOFC and Steam Turbine based Integrated Power Plant at Ashuganj Power Station Company Limited," *2019 5th International Conference on Advances in Electrical Engineering (ICAEE)*, Dhaka, Bangladesh, 2019, pp. 269-274, doi: 10.1109/ICAEE48663.2019.8975584.